

Reviewers' comments are italicised, our response is not. Our direct actions are highlighted in red text. Line numbers refer to the marked-up version of the manuscript

Reviewer 1.

The Ms "Pingos as hot spots of methane emissions" is a very interesting ms about the groundwater flow related to the special features of pingos. The Ms is very well written, the results are presented and discusses in concise manner. Almost perfect... Only one major drawback I realized at the end of the study: The emissions or flux of methane from a water body (river, sea, lake) is related to the difference between the measured concentrations (C_w) and the equilibrium concentration (C_{equ}) of methane in this water; and the gas-water transfer velocity (k). $J = (C_w - C_{equil}) \times k$ Thus, the calculation and assumptions drawn are wrong, and this part has to be corrected! Also, the way the flux / emission is finally calculated should be explained in the M&M section.

We appreciate the positive comments and acknowledge that the perceived drawback related to our flux calculations needs to be addressed in the paper. Since no comments other than the flux calculation issue require consideration, we deal only with this point below.

Our manuscript acknowledged that it “crudely” estimates the methane release from pingo waters to the atmosphere. It did so by assuming that all waters achieve equilibrium with the atmosphere due to turbulence and freezing effects. This is further simplified by the fact that the equilibrium concentration is negligible compared to the initial concentration and so can be ignored. The equation given by the reviewer is most relevant for cases where equilibrium is not achieved – for example with standing water bodies like lakes, or the sea, with a continuous influx and significant residence time caused by storage. However, envisage a turbulent spring flowing without such storage in a pond, and freezing while it does so. These conditions render the above calculations rather unsuitable, and they fail because the coefficient k is impossible to define. A further issue is that the proposed method does not account for the ebullition of gas, and so might underestimate the gas flux. The reviewer’s comment is valid for one or two of our sites during the summer though, and we completely accept this criticism. In fact we have already employed the recommended approach in a different paper about one of these sites (Hodson et al, 2019). **Given these uncertainties, we took the Editor’s advice and presented a more qualitative argument about the likely importance of the fluxes to the atmosphere. Further details are below – but note the extensive changes to Section 4.3.**

Reviewer 2.

We thank the reviewer for also complementing the paper for being and well-written.

The development of an open system pingo should be explained in more detail. It was unclear to me, how liquid water may find it’s way through the permafrost. What is the temperature of the permafrost? Are these open system pingos particularly

developing above marine sediments? What is the difference to a 'normal' pingo? It's particular difficult to understand since the cited reference (L57) is not given in the list of references.

The citation, which describes the formation process for lagoon Pingo has been corrected (line 58). Since only a brief description about formation is given in the introduction (lines 58 – 61), more comments on the Adventdalen pingos are included in Section 2.1 (lines 73 – 81), where there are three further citations. Unfortunately, we do not know the temperature of the permafrost in this area.

Furthermore, more background information should be given on the geology of the study sites, including the geology of the surrounding mountains that may affect the composition of the spring water. Is there a connection between the springs and fresh meltwater (as suggested in lines 275ff)? Is there a talik below the river and might this be connected to the springs?

We acknowledge the need for more background information regarding the genesis of the pingos, the geology and the type of methane that might be present. This information is now included in the field site section, in lines 95 onwards. We also improved the representation of the geology in Figures 1 included a new Figure 2b – all described from lines 95 to 108. Two new citations have been included too. From lines 110 to 117, we have used new citations and added additional text (some of which was originally described in “Section 2.4: Other data resources”) to better integrate existing knowledge into the description of the field site. The discussion also uses this information to explore the links between the shale unit and the geochemistry, due to the unusual observations at River Bed Pingo (distal site) in 2017 (line 297 onwards).

Furthermore, more background information on the potential source of the methane in the spring water should be given. The authors differentiate biogenic and geogenic sources. However, it should be made more clear which geogenic sources might be present, gas hydrates or natural gas from deep deposits? Is there information on these sources in the region, and what is the carbon stable isotope signature of these sources?

We have included more information in the above section between lines 110 – 117. Since hydrates could be composed of any gas origin (ie bio or geo-genic) and since it is not known if any are indeed present in the valley, we decided not to discuss hydrates in the introduction.

Concerning the biogenic source, it should be explained why high methane concentrations in marine waters are expected. Generally, no methane is produced as long as sulfate is present. In contrast, methane, e.g. from gas hydrates is oxidized with sulfate as electron acceptor.

The reviewer raises a good point here on account of the potential for sulphate reduction to out-compete methanogenesis. We made the point because Cl correlates with methane concentrations. We now think other processes could cause this and so we have removed this point.

The discussion concerning the methane sources is rather speculative due to a lack of data. The carbon stable isotope signature is only a weak indicator for differentiating geogenic and biogenic methane sources. If only the carbon stable isotope signatures of methane are available and no delta D or concentrations of further hydrocarbons, as in this manuscript, no differentiation between geogenic and biogenic sources is possible. E.g., gas hydrates may have carbon stable isotope signatures between about -40 and -70‰ a range covering the whole values given in this manuscript.

The reviewer implies that our discussion about methane provenance is weak because it is entirely based upon $^{13}\text{C}-\text{CH}_4$. The reviewer then implies that we cannot discriminate between geogenic methane, biogenic methane and hydrates. But hydrates are not a source of methane – they are a transient store of either geogenic or biogenic methane (or a mixture of the two). We therefore seek only to assess whether there is any evidence for geogenic methane in the water, largely because previous work has demonstrated a clear dominance of biogenic methane just beneath the permafrost at our field site. As a result, we respectfully suggest that there is no need for the $\text{dD}-\text{CH}_4$ isotopes because:

- i) $^{13}\text{C}-\text{CH}_4$ alone can rule out geogenic when the values are low, and we have many low values that fall outside this “geogenic range”.
- ii) An earlier study of methane in pore spaces conducted at our site uses CH_4 concentrations, $\delta^{13}\text{C}-\text{CH}_4$, $\delta^{13}\text{C}-\text{DIC}$ and the presence of other hydrocarbons to establish the relative abundance of biogenic versus geogenic methane from the surface down to ca. 900m (Huq et al, 2017). This work clearly shows that the geogenic methane fails to migrate effectively into the aquifer beneath the permafrost. This work does not require delta-D because the presence of other hydrocarbons is used as a reliable indicator of geogenic CH_4 instead (Huq et al, 2017). This information is included in Figure 4.
- iii) The above study shows that there is a methane source in an aquifer immediately below the permafrost that is largely biogenic.
- iv) The biogenic methane inferred from Huq’s study was also found by a mining company, who reported a salty groundwater body just beneath the permafrost with a $^{13}\text{C}-\text{CH}_4$ range (-48.9 ‰ to -52.9‰) that is almost identical to that found at our nearby pingos sites (ie River Pingo and Innerhytte Pingo: -49.7 ‰ to -57.8‰ as in Table 2). Their reported salt content was 1500 mg/L, which is also almost identical to that found at these two pingos (1380 –1540 mg/L: Table 1).
- v) At the other two pingo sites, the $^{13}\text{C}-\text{CH}_4$ values either lie within the same range as the above, or are even lower (more ^{13}C depleted) and therefore too low to be geogenic.

We therefore conclude that there is almost no evidence for a significant geogenic methane contribution to our springs. **We have edited lines 250 - 261 and Figure 4 to make incorporation of these other data clearer and more compelling. We also included reference to our new publication about the deeper geogenic gas (Ohm et al, 2019).**

But the weakest part of the discussion is the part on the pingos as methane emission hotspots. The authors derive spring water fluxes from an unpublished study on Adventdalen's groundwater system, add unpublished data on methane concentrations in a 'neighboring lake', which contributes about 1/3 to the total flux estimate and assume that 100% of the methane in the water will be emitted to the atmosphere. Estimating methane fluxes from water concentrations comes along with high uncertainties. It might be possible for pond, lake or sea water. However, in soils, bacteria will likely oxidize a large fraction of the methane as soon as oxygen is available. Hence, methane fluxes will likely be much lower. To derive meaningful data on methane fluxes from soil surfaces, emission measurements should be conducted.

We tend to agree that the emission estimates are the weakest part of the paper, but feel that their potential significance should still be addressed. **We have therefore followed both the reviewer's and the editor's suggestion to achieve this with a more qualitative approach, which is now described between lines 344 – 348.**

However, since we respectfully disagree with some of the criticisms directed towards our emission estimates, we first wish to offer the following explanation (that could have been clearer in our initial manuscript):

Methane consumption in soils "will likely oxidize a large fraction of the methane as soon as oxygen is available".

We point out that soils are frozen for much of the year, yet the springs we study are constantly discharging, usually over a smooth ice surface. Furthermore, we seldom find the springs infiltrating into soils before much of their methane has been lost. In summer, the springs erode turbulent channels through impermeable marine clays or cascade down the flank of the pingo – which is also conducive to rapid degassing to the atmosphere but not really to methanotrophy. However, at pingos where lakes form upon their summit, then methanotrophy is indeed more likely. **These points have been incorporated into the new Section 4.3 along with some new empirical evidence and a new figure (Figure 5) (see lines 371 - 404) that demonstrates rapid methane loss.**

To derive meaningful data on methane fluxes from soil surfaces, emission measurements should be conducted.

We do not wish to derive such data because we are describing emission from springs, not soils. Our springs by-pass the soil environment. We hope that the new text described above helps clarify this

The authors derive spring water fluxes from an unpublished study on Adventdalen's groundwater system...

This study is Hornum et al, currently under revision and available to the reader as a discussion paper. It provides a lot of necessary background data, but **we have greatly reduced the dependence upon this paper (at the Editor's request) and have made the whole section simpler and easier to follow. All speculation about springs not sampled in our study has been removed. One additional site, "Lagoon Lake" has been included though, because it is clearly part of the Lagoon Pingo system, and we present sufficient measurements from this site to justify its inclusion (lines 360 – 362). Table 3 has been changed and the source of the information used for the fluxes made clear in the caption.**

Furthermore, there seems to be a mistake in the calculation of the land fluxes from Adventdalen valley using the Pirk et al. (2017) paper and the active layer fluxes seems twice as high (see specific comments) as given in this manuscript. In this case the relative contribution of the sub-permafrost fluids is reduced by 50%.

We regret that the reviewer has made a mistake – which is easy to do on account of the wording in the Pirk paper. **This issue is dealt with under specific comments below.**

Furthermore, the winter fluxes are not considered in these estimates, which might be as high as the summer fluxes (see Zona et al., 2016).

The Pirk et al (2017) study does in fact include the freeze-up processes that were emphasised by Zona et al's (2016) study. After this period, the (late) winter emissions in Adventdalen have not been studied much, although Pirk et al (2016) did some pre-melt chamber work one April/May and found great suppression of the methane flux by icing layers. Where such layers were less prolific (in Zackenberg, Greenland – not Svalbard), the winter fluxes were one to two orders of magnitude lower than those before the end of freeze up. Therefore, no amendments to the manuscript were deemed necessary concerning this point.

Concluding, I suggest changing the title of the manuscripts, since it indeed does not measure methane emissions. Furthermore, I would downplay the calculations of methane emissions and more clearly consider their uncertainties. The authors mention that it is only a 'crude' estimate, which is correct. In this case, this crude estimate should not be in the focus of the manuscript by mentioning it in the title and elaborating it over more than half of the discussion. The authors may discuss the emissions in a more qualitative way and also include information about the abundance of such springs, if available.

We have changed the title to better reflect the role of the pingos and have also changed the signposting at the end of the introduction section to emphasise that the paper is largely about the exploitation of pingos by the gas-rich fluids (line 62 to 70). We have also changed the emphasis of Section 4.2 to remove emission estimates.

Finally, the reference list needs attention.

Done

Specific comments:

L31: This quote does not fit here very well, better cite particular studies that are 'quantifying the release of methane from the active layer during summer thaw' and not a general review on the permafrost carbon feedback.

A new citation has been added that incorporates active layer emissions and methane cycling into a global review. I changed the sentence to make the lack of explicit active layer studies acceptable.

L57: This reference is not given in the list of references

The citation has been corrected (see line 58)

L138 ff: How were gas pressures measured in the vials and which CH₄ solubility was assumed?

Details of the number of standards, the linear calibration range used and the detection limit are now included lines 171 - 174. The analytical process does not measure pressure as no pressurisation occurs during headspace formation. Appropriate amendments have been made to the text to make this clear (line 169). We use the Bunsen Solubility Coefficient (a proxy for gas solubility) to account for temperature effects upon the solubility value.

L214: Excess CO₂ seems to correlate with methane concentration not it's variation.

Changed (line 239)

L225f: What means 'overlaps closely'?

Changed (on line 250)

L239ff: The last part of this paragraph belongs to the discussion.

Done. See deletion from line 269

L258ff: The 'distal' samples not only seem to be different but they very obviously are.

Sorry, there might be some British understatement in here. We have completely changed how we introduce these "distal samples" because it is now obvious to us that they aren't linked to the pingo like we thought they might have been. See lines 134 and then again in the results (lines 213 - 215) and discussion (lines 280 -286).

L265ff: I find this paragraph confusing and the conclusions not convincing. It is indeed counterintuitive to expect that the influence of marine waters are higher the farther one comes from the sea. Furthermore, this conclusion is only supported if a part of the dataset (distal samples) is omitted from the analysis, but there is no justification given to do so.

We felt we simply cannot ignore the strong influence of sea water upon the methane concentrations that is made obvious by our results. The likely causes of the counter-intuitive Cl⁻ gradient are explained in our companion paper (Hornum et al, TC Discussions) and have been addressed in lines 295 - 301. We have also worked hard to justify the omission of the River Bed

Pingo Distal samples throughout the paper (see above), after realising that we had done a poor job of explaining it in the first manuscript. However, it is perfectly reasonable to do this in our opinion.

Furthermore, it is unclear why the system is more diluted downstream by fresh groundwater from snow and ice melt.

The system is increasingly diluted by fresh groundwaters because the valley is flanked by plateau highlands (line 301 and Figure 2a). See also response to next point.

I understand, also from Fig. 4 that the sampled water originates from below the permafrost. In this case, the up-valley sites should be more influenced by melt water.

Not really. The permafrost thicknesses are greater inland, so waters could be emerging from greater depths. This means the likelihood of denser, more saline springs increases inland. The issue is discussed at length in Hornum et al and so we feel uncomfortable extending our discussion to cover all of this hypothesis. However, we hope that the substantial amendments from line 295 cover the matter sufficiently without heavy reliance upon Hornum et al (In Review) at the request of the Editor.

L286ff: The explanation of the variability in CH₄ stable isotopes is unclear. Why should CH₄ oxidation preferentially take place while the fluids are trapped below an ice lid and not during its transport to the surface or after surface thaw?

We argue that rapid switching in the source signature of the methane arriving at the pingo is unlikely because the system has a constant flow and long residence time. Rapid switching to ¹³C-enriched methane therefore seems most likely to be caused by the variable outburst cycle from beneath the ice blisters that form on the pingos. Methane gradually oxidises beneath the lid, then outbursts and refills once more, allowing “fresh” methane to mix with any residual “old” methane. Since the outbursts occur i) from different elevations on the pingo (thus emptying the ice blister to different degrees), and ii) after different storage times beneath it, the variability in ¹³C results from different mixing ratios between “fresh” and “old” methane at the time of sampling. It is unlikely that oxidation occurs during transport to the surface because the process is rapid compared to the storage time beneath the ice lid. Far less oxidation effects are therefore apparent in summer, when no such storage exists. See lines 311 – 323. Some oxidation prior to the ascent to the surface is also described in the discussion ending on line 340.

To oxidize methane, an electron acceptor is needed, the respective microorganisms and liquid water but not stagnant water. And what might be the electron acceptor for methane oxidation? The fluids seem mostly oxygen free and low in sulfate.

We appreciate the comments here. We will describe methanotrophy in a forthcoming paper, which has found that it occurs in the marine muds (at Lagoon Pingo and Forstehytte Pingo) but not the shale rock debris mantle on Innerhytte and River Pingos. We think it is beyond the scope of the present paper to describe this molecular work here, not least because we have found a novel organism at Lagoon Pingo. It will also support our assertions about why ¹³C-CH₄ signatures at Lagoon+Forstehytte Pingos differ to Innerhytte+River Bed Pingos.

L310: What means 'favorable thermodynamic conditions' in this context? Favorable for which process?

The comment has been removed.

L317ff: I understood from L286ff that the springs are frozen in winter. Please clarify.

Partial freezing of the springs in winter forms an ice lid. This gradually expands upwards, then fractures and releases the spring water. It then flows over ice, releases methane and refreezes to form an icing. We regret not describing these processes further and have included appropriate text to describe what happens on lines 122 - 127

L 331FF. Please give the reference for 'this paper'. Furthermore, clarify to which paper the newly introduced data from the 'neighboring lake' belong.

Done (re proper reference of Hornum et al, TC Discussion paper). The additional data were the authors' own observations from just prior to submission and methane levels and dates of sampling are included in the text (line 360).

L345: Pirk et al., 2017?

Yes, corrected

L347f: This calculation neglects aerobic methane oxidation, which might oxidize up to 100% of the methane before it is released into the atmosphere. Hence, the flux assumption from the springs is the upper limit of methane fluxes from the springs.

We agree it is an upper estimate, but would like to point out that 100% removal is impossible in the system under study. We have changed the emphasis of the discussion to avoid direct discussion of emission (see earlier comments and lines 344 - 348)

L363: Pirk et al. (2017 not 2018) report 'typically...a...seasonal budget of around 2gC m⁻²' (not 1 g C m⁻²) for the summer thaw season (1st June to 30th September) in Adventdalen. According to my calculation the annual flux from 4.7 km² would then be about 12,600 kg methane yr⁻¹ (not 6,040 kg methane yr⁻¹).

Citation corrected. The quote from the Pirk et al paper unfortunately refers to the median of two sites: Adventdalen and Zackenberg (in Greenland). The emissions from Zackenberg are greater than those from Adventdalen. Quick scrutiny of Figure 5 in Pirk et al (2017) clearly shows that all of the median values at Adventdalen lie below 2. It is therefore hard to justify using 2 gC m⁻² y⁻¹ as a spatially representative value (not least because it includes data from elsewhere). For this reason, I digitised Figure 5 in Pirk et al and determined the minimum and maximum median values from their three year study. These values were used to produce the range of likely emissions from wetlands for comparison with our emission estimates from springs. This range is presented in Table3.

Furthermore, the winter fluxes are not considered in these estimates, which might be as high as the summer fluxes (see Zona et al., 2016).

We have responded to this above.

L375f: The meaning of this sentence ('The sensitivity...') is unclear.

Appropriate amendments to this sentence and the next.

L376ff: I cannot follow this calculation. Where does the number 50 L sec-1 come from? What is the Adventdalen terrestrial methane flux? In addition, why compare the total annual runoff of Adventdalen with the groundwater flux of 50 L- sec-1? The authors are aware that the methane concentration in surface melt water is several orders of magnitude lower than what they found in the springs with sub-permafrost fluids. This comparison is without meaning.

We intended a straight-forward discussion of the sensitivity of potential methane emissions to a change in the water budget here. Every river has a baseflow largely driven by groundwater. Here we have just 1.6 L/s of sub-permafrost groundwater contributing to baseflow. Literature argues that the amount is likely to increase (citation of Victor Bense's work, who has been consulted directly). We therefore demonstrate that for an increase to 50 L/s then the flux of methane available for emission from the entire valley could increase by five times. Although 50 L/s seems high relative to the situation at the moment, it would still only represent 0.001% of total annual runoff. Most watersheds have a far higher degree of groundwater flow contributing to total runoff, but this is continuous permafrost terrain. **Appropriate amendments have been made to the paragraph (lines 412 – 419) to help explain the purpose of this paragraph. Note that the criticism deserves less attention now that we have decided to not attempt a direct emission estimate.**

Table 2: Please also differentiate the "distal" samples from the River Bed Pingo

Done

Fig. 2 is difficult to read. Please give references for the published pore water data and please use units that make a comparison with the data in the tables possible (e.g. mgL-1 not μ L mL-1)

We appreciate that the diagram (Figure 4) needs time to understand properly and have tried once more to make it less cluttered with some edits. However, the units cannot be changed because the graph brings in pore gas analyses for comparison to our aqueous concentrations.

1 Open system pingos as conduits for highly concentrated methane seepage in Svalbard

2 Andrew J. Hodson^{1,2}, Aga Nowak¹, Mikkel T. Hornum^{1,3}, Kim Senger¹, Kelly Redeker⁴, Hanne H.
3 Christiansen¹, Søren Jessen³, Peter Betlem¹, Steve F. Thornton⁵, Alexandra V. Turchyn⁶, Snorre
4 Olausen¹, Alina Marca⁷

5
6 ¹Department of Arctic Geology, University Centre in Svalbard (UNIS), N-9171 Longyearbyen, Norway.

7 ²Department of Environmental Science, Western Norway University of Applied Sciences, Røyrgata 6, N-6856 Sogndal,
8 Norway

9 ³Department of Geosciences and Natural Resource Management, University of Copenhagen, 1350 Copenhagen K, Denmark.

10 ⁴Department of Biology, University of York, YO10 5DD, UK.

11 ⁵Department of Civil and Structural Engineering, University of Sheffield, S10 2TN, UK.

12 ⁶Department of Earth Sciences, University of Cambridge, CB2 3EQ, UK.

13 ⁷School of Environmental Sciences, University of East Anglia, Norwich, NR4 7TJ, UK.

14

15 *Correspondence to:* Andrew J. Hodson (AndrewH@unis.no)

16 **Abstract.** Methane release from beneath lowland permafrost represents an important uncertainty in the Arctic greenhouse gas
17 budget. Our current knowledge is arguably best-developed in settings where permafrost is being inundated by rising sea level,
18 which means much of the methane is oxidised in the water column before it reaches the atmosphere. Here we provide a different
19 process perspective that is appropriate for Arctic fjord valleys, where local deglaciation causes isostatic uplift to out-pace rising
20 sea level. We show how the uplift induces permafrost aggradation in former marine sediments, whose pressurisation results in
21 methane escape directly to the atmosphere via ground water springs. In Adventdalen, Central Spitsbergen, we show how the
22 springs are historic features, responsible for the formation of open system pingos, and capable of discharging brackish waters
23 enriched with high concentrations of mostly biogenic methane (average 18 mg L⁻¹). Thermodynamic calculations show that
24 the methane concentrations sometimes marginally exceed the solubility limit for methane in water at 0 °C (41 mg L⁻¹). With a
25 combined discharge of just 1.6 L s⁻¹, four pingo springs transport a flux (1050 kg CH₄ a⁻¹) equivalent to between 10 and 17%
26 of the methane emissions measured in local wetlands. This confirms that sub-permafrost methane migration deserves more
27 attention for improved forecasting of Arctic greenhouse gas emissions.

28 1 Introduction

29 Methane evasion to the atmosphere from thawing Arctic permafrost represents a significant risk to future greenhouse gas
30 management, and so great emphasis has been placed upon quantifying the global importance of methane release from the
31 active layer (see [Dean et al, 2018](#)). However, the potential for methane evasion from deeper sub-permafrost sources also exists
32 (Anthony et al, 2012; Betlem et al, 2019; Kohnert et al, 2017), but since the means by which the gas by-passes the permafrost
33 are unclear, their possible timing, magnitude and impact are very uncertain. Recent research has provided significant insights

34 into the role of landscape change and methane release from low relief Arctic shelf environments typical of the Canadian,
35 Siberian and North Alaskan coastlines (Kohnert et al, 2017; Frederick et al, 2016; Dmitrenko et al, 2016). Here, sea level
36 inundation has enhanced methane escape by inducing permafrost thaw (Frederick et al, 2016). However, this mechanism is
37 not relevant to many fjord coastlines in the Arctic because isostatic uplift has out-paced sea level rise (Dutton et al, 2015).
38 Here, the uplift of sediments deposited in the fjord since the Last Glacial Maximum (LGM) has caused their exposure to the
39 atmosphere, resulting in a period of freezing and permafrost aggradation (e.g. Cable et al, 2018; Gilbert et al, 2017, Gilbert et
40 al, 2018). Fjord coastlines which have undergone significant isostatic uplift are typical of Svalbard, Novaya Zemlya, northern
41 Greenland and the Canadian Arctic archipelago. It is therefore significant that these areas are poorly represented in our current
42 understanding of pan-Arctic methane emissions from the land surface.

43

44 Fjords are notable for some of Earth's most rapid rates of sedimentation and organic carbon burial during glacial retreat,
45 producing thick sediment sequences potentially conducive to biogenic methane production (Smith et al, 2015; Syvitski et al,
46 1986; Włodarska-Kowalczyk et al, In Press). In addition, the rocks underlying many Arctic fjords support either proven or
47 highly probable natural gas resources (Gautier et al, 2009). Therefore methane from geogenic sources such as coal beds and
48 shale is also likely to be present. At the LGM, widespread methane hydrate stability zones were present under the ice sheets,
49 providing a transient reservoir for both the biogenic and geogenic methane. The warmer period that caused the onset of ice
50 sheet retreat after the LGM caused the gas hydrates to become thermodynamically unstable, and the methane began to escape
51 rapidly through the recently uncovered sea floor (Crémière et al, 2016; Smith et al, 2001; Weitemeyer and Buffet, 2006).
52 Evidence for such rapid fluid escape include pockmarks (Crémière et al, 2016; Portnov et al, 2016) (Figure 1a), whose
53 occurrence in Svalbard is particularly well-documented because some of them remain active today (Liira et al, 2019; Sahling
54 et al, 2014). Sea floor methane emissions are subject to very significant removal processes due to dissolution and oxidation
55 within the overlying water column (Mau et al, 2017). Further, Pohlman et al (2017) have shown that sea floor gas emissions
56 in coastal waters off Svalbard may also be offset by far greater rates of atmospheric CO₂ sequestration into the overlying
57 surface waters, because the rising bubbles help nutrient-rich bottom waters rise up to fuel the photosynthesising plankton
58 community. However, Hodson et al (2019) showed that pockmarks exposed by isostatic uplift have the potential to form
59 methane seepage pathways on land. Since any groundwater carrying the gas through the permafrost will be subject to freezing
60 temperatures, these features are likely to become discernible as small, ice-cored hill forms known as open system pingos
61 (Figure 1b). Therefore, pingos and other terrestrial seepages must be considered as migration pathways through what is
62 otherwise regarded as an effective seal or "cryospheric cap" formed by the permafrost (Anthony et al, 2012). Such routes
63 potentially represent the most harmful greenhouse gas emission pathway for methane trapped beneath permafrost, because gas
64 can escape directly to the atmosphere without removal by oxidation within the overlying water column of the fjord.

65

66 This paper therefore investigates how methane-rich fluids readily escape from beneath permafrost by exploiting the open
67 system pingos that have formed following isostatic uplift and permafrost aggradation in Svalbard's fjord landscape. We show

68 that the pingos form natural “hotpots” for the ventilation of sub-permafrost methane directly to the atmosphere, with the
69 potential to account for a meaningful proportion of the total annual methane emissions in Adventdalen, a representative, well-
70 researched fjord valley system in Central Spitsbergen, Svalbard.

71 **2 Methods**

72 **2.1 The field site**

73 Adventdalen’s open system pingos are located in a lowland valley that has been rapidly in-filled by a pro-grading delta system
74 throughout the Holocene. This was driven by ice sheet retreat commencing ca. 11 000 years ago (Gilbert et al, 2018) and is
75 represented by the landscape model in Figure 1. As with many open system pingos in Central Spitsbergen, their formation was
76 intricately linked to changes in groundwater dynamics that occur after such deltaic sediments emerge from below sea level and
77 start to freeze. This permafrost aggradation increases hydraulic pressure and thus forces residual groundwaters toward the land
78 surface. Since the hydraulic conductivity of the fine-grained, uplifted marine sediments is very low (Toft-Hornum et al, In
79 Review), the fluids are likely to exploit any former pockmarks that are uplifted with them (e.g. Hodson et al, 2019). Further
80 freezing near the surface then results in expansion and the formation of a small hill with an ice core, or “pingo” up to 40 m
81 higher than the surrounding topography (Liestøl, 1996; Yoshikawa et al, 1995; Yoshikawa, 1993). Figure 2a shows that two
82 pingos (Lagoon Pingo and Førstehytte Pingo) are situated in the lower part of the valley, whilst two others (Innerhytte Pingo
83 and River Bed Pingo) are up-valley, and just beyond the former marine limit at ca. 70 m asl. Lagoon Pingo, nearest to the
84 coast, is thought to be less than 200 years old, and has had springs documented from as early as 1926 (Liestøl, 1996; Yoshikawa
85 and Nakamura, 1996). At Førstehytte Pingo, a spring has also been known to exist since the 1920’s, but the pingo is thought
86 to be much older. Radio-carbon dates for molluscs in the marine sediments uplifted by the Førstehytte Pingo give a maximum
87 age limit of 7000 ± 70 years (Yoshikawa, 1993; Yoshikawa and Nakamura, 1996). Innerhytte Pingo and River Bed Pingo are
88 of unknown age, and since they lack a cover of marine sediments containing mollusc shells, no radiocarbon dates are available.
89

90 Like many fjord valleys, the rate of sedimentation was extremely high during ice sheet retreat, and so a “wedge” of up to 60
91 m of valley in-filling has occurred within the former marine limit (Cable et al, 2018; Gilbert et al, 2018). However, the
92 permafrost in the valley floor of Adventdalen is up to 120 m thick, so much of the fine sediments have frozen since their
93 exposure by isostatic uplift during the Holocene, with the exception of the sediments closest to the contemporary shoreline
94 and pockets of saline “cryopegs” further up-valley (Keating et al, 2019). There are no taliks beneath the river, because river
95 discharge volumes drop rapidly in late August and allow freezing to commence early in the winter. Although the typically
96 fine-grained, frozen marine sediment infill in the valley has a low hydraulic conductivity, the underlying glacial tills, and in
97 particular the upper (unfrozen) geological strata beneath that, both seem to support important sub-permafrost fluid migration
98 pathways (Huq et al, 2017; Hornum et al, In Review: Figure 2b). Unique insights into the sub-permafrost geology were
99 provided by the legacy of geological exploration in the region, currently managed by the Store Norske Spitsbergen Kulkompani

100 (SNSK). This provided unpublished borehole records and geochemical data that allowed us to better understand the presence
101 of methane and groundwater beneath the permafrost. Furthermore, geochemical and geophysical analysis of deep rock cores
102 have also been undertaken in the valley as part of the UNIS CO₂ Project (Braathen et al, 2012; Olausen et al, 2019). Key sites
103 for these earlier investigations are shown in Figure 2a. Of particular importance are the permeable, fractured sandstones of the
104 Lower Cretaceous Helvetiafjellet Formation immediately beneath the permafrost westwards of Innerhytte Pingo, and a ca. 400
105 m-thick Lower Cretaceous to Middle Jurassic mudstone-dominated succession beneath that (the Rurikfjellet and Agardfjellet
106 Formations). The mudstone succession also outcrops eastwards from Innerhytte Pingo, as well as to the north at the base of
107 the mountains (see cross section, Figure 2b). Fractured, uplifted mudstone clasts therefore form the mantle lying over the
108 Innerhytte and River Bed Pingos, whilst younger marine muds form the mantle over Førstehytte and Lagoon Pingos.

109
110 Earlier work has shown that the fractured sandstones host an important, biogenic methane-rich aquifer, whilst the mudstones
111 form an effective flow boundary that seems to suppress the upward migration of its own geogenic methane resource (Huq et
112 al, 2017). The gas-rich upper sandstone aquifer therefore contains few hydrocarbons other than methane, whilst in the lower
113 mudstone successions, ethane and propane have been detected at levels indicative of a geogenic gas source (Huq et al, 2017;
114 Ohm et al, 2019). Fluid migration through the outcropping mudstones to Innerhytte and River Bed Pingos is therefore likely
115 to exploit faults (shown conceptually in Figure 2b, but very poorly understood), whilst fluid migration towards Førstehytte and
116 Lagoon Pingos is likely to exploit the fractured sandstones of the Helvetiafjellet Formation and glacial tills immediately
117 beneath the permafrost (Figure 2b).

118
119 Four of six open system pingos in Adventdalen discharge groundwaters all year (Figure 2). In the summer, the springs are
120 discernible as a discrete conduit discharging either into the base of a small pond (e.g. Lagoon Pingo), directly out of the pingo
121 and down its flank (Førstehytte Pinge, Innerhytte Pingo) or straight out of the base of the pingo and into the Adventelva river
122 bed, which may or may not be flooded due to its braided nature (River Bed Pingo). During summer, surface meltwater flooding
123 in the valley hinders access to the pingos, since the river must be crossed to gain access. At other times of the year, after
124 freezing has commenced (usually late September until mid-May), spring water accumulates beneath a large ice blister. The
125 pressure caused by continuous flow expands the ice blister, forcing its summit upwards by as much as 4 m by the end of winter.
126 The expansion is periodically checked by turbulent outbursts of water that typically freeze within 100 m of the pingo. All four
127 springs were sampled before the melt season after drilling up to 2 m through their winter ice cover, releasing pressurised flow.

130 **2.2 Fieldwork**

131 Field work involved consecutive spring-time sampling campaigns (March - April) at the four pingos from 2015 until 2017. In
132 addition, opportunistic sampling at the pingos was conducted in summer 2017, where low river levels made access to the field

133 sites possible. We focussed our sampling on the larger, discrete springs that were closest to the pingo summit, but in 2017 the
134 spring that was sampled at River Bed Pingo was in a different location to previous years (away from the foot of the pingo).
135 This site is hereafter referred to as “River Bed Pingo Distal” and is discriminated for reasons that become apparent when our
136 results are considered.

137
138 Pingo springs were sampled after drilling up to three metres through their winter ice cover using a 7 cm diameter Kovacs drill
139 and Stihl two-stroke engine. Although the icing surfaces were sometimes visibly cracked, with an outflow of water, drilling
140 was still employed to reduce the likelihood of oxygenation before sampling and contamination from local snow. At the
141 sampling site, pH, temperature, dissolved oxygen and Oxidation-Reduction Potential (ORP) were recorded using Hach Lange
142 HQ 40D meters and dedicated electrodes/sensors. These were calibrated prior to use with the exception of the dissolved O₂
143 measurement, which was conducted using the luminescence method and thus used a factory calibrated sensor tip. To prevent
144 freezing problems and electrode malfunction, water samples were pumped through a bespoke, air-tight flow cell with an
145 internal heating element maintaining the sample flow at ca. 7 °C.

146 **2.3 Analytical work**

147 Samples for dissolved iron and manganese analysis were syringe-filtered immediately in the field through 0.45 µm filters into
148 pre-cleaned 15 mL Eppendorf Tubes, before acidification to pH ~ 1.7 using reagent grade HNO₃⁻ (AnalaR 65% Normapur,
149 VWR, IL, USA). The analysis of dissolved Fe and Mn was then completed using Inductively Coupled Plasma Mass
150 Spectrometry or ICP-MS (PerkinElmer Elan DRC II, MA, USA). Precision errors of the analyses were < 5% according to
151 repeat analyses of mid-range standards, with a detection limit of 1.0 µg L⁻¹. No contaminants were detected above this limit in
152 the analyses of blank deionised water samples. Samples for major ion analysis (here Ca²⁺, Mg²⁺, Na⁺, K⁺, Cl⁻, NO₃⁻, SO₄²⁻)
153 were also filtered in the same manner (but not acidified) and stored in 50 mL Corning centrifuge tubes after being triple rinsed
154 with filtrate. The analysis was conducted on Dionex DX90 Ion Chromatographs with a detection limit of 0.02 mg L⁻¹ for the
155 lowest, undiluted analysis. Precision errors for these ions were all <5% for mid-range standards.

156
157 Charge balance calculations were used to provide the indicative values of HCO₃⁻ and CO₃²⁻, given (as DIC or dissolved
158 inorganic carbon) in Table 1. Excess CO₂ levels were estimated from calculations of the partial pressure of CO₂ using the
159 online WEB-PHREEQ Geochemical Speciation Software (<https://www.ndsu.edu/webphreeq/>).

160
161 Samples for the determination of dissolved methane and carbon dioxide concentrations as well as δ¹³C-CH₄ and δ¹³C-DIC of
162 the waters were taken directly from the spring following immersion, complete filling and sealing of a 22 mL Wheaton bottle
163 with a crimp-top lid with septum. The samples were stored inverted under water at 4°C until analysis. The analysis of the CH₄
164 was performed by gas-chromatography on a Shimadzu GC-2014 instrument equipped with a methaniser and flame ionisation
165 detector, using a 30 m GS-Q, 0.53 mm internal diameter column with N₂ as a carrier gas at a flow rate of 8 mL/minute, and

166 injection, oven and detector temperature of 60, 40 and 240 °C, respectively. The sample size was 100 µL and the sample run
167 time was 3 minutes at 40 °C. Concentrations of dissolved CH₄ were obtained according to a mass balance calculation for the
168 samples (McAuliffe, 1971), in which a known volume of N₂ was injected into sample vials to create a headspace whilst
169 allowing sample displacement through an outlet needle to prevent pressurisation (Tyler et al, 1997). After shaking and
170 equilibration (2 h) the CH₄ partitioned into the headspace was analysed by GC-FID and the corresponding mass in the gas and
171 aqueous phase was determined by Henry's law, to obtain a final concentration in the water sample. Six calibration gas
172 standards were prepared on the day of analysis by serial dilution of certificated 60% CH₄: 40% CO₂ mixed gas using O₂-free
173 N₂ as the balance gas. The calibration was linear across the range 0 – 140000 ppm v and the detection limit equivalent to ~
174 0.017 mg L⁻¹. Repeat analyses of mid-range standards indicated a precision error < 1.3%.

175
176 Analysis of dissolved methane isotopic composition and concentration was performed using the gas headspace equilibration
177 technique (Magen et al, 2014) (5mls sampled water were injected into a Viton-stoppered, He-flushed 120 mL glass serum
178 vial). 10mls of the headspace was then flushed through a 2 mL sample loop, and injected onto a 25 m MolSieve column within
179 an Agilent 7890B GC attached to an Isoprime100 Isotope Ratio Mass Spectrometer (IRMS) (Tyler et al, 1997). Analytical
180 precision errors for samples > 3 ng-C were better than 0.3‰ for isotopic values, and < 3.5% for concentration, based on
181 methane standard injections. δ¹³C_{DIC} was measured by a Continuous Flow Isotopic Ratio Mass Spectrometer (Thermo-
182 Finnegan Delta V with gasbench interface) and an error of 0.1‰. All δ¹³C_{DIC} and δ¹³C_{CH₄} values are reported vs. the Vienna
183 Pee Dee Belemnite standard.

184
185 Samples for water isotope analysis were collected as unfiltered 20 mL aliquots in a screw-top HDPE bottle. The bottles were
186 subsampled into 1.5 mL vials with septa closures and loaded into the auto-sampler tray of a CDRS instrument (Picarro V 1102-
187 i model). Each sample was injected and measured 6 times using 2.5 µL of water for each injection. Together with the samples,
188 two secondary international standards (USGS 64444 and USGS 67400) and one internal laboratory standard (NTW – Norwich
189 tap water) were measured, each injected 10 times in order to minimise memory effects. Final isotopic compositions were
190 calculated using the calibration line based on the secondary international standards and reported in ‰ units with respect to V-
191 SMOW on the V-SMOW – SLAP scale. The precision error of the measurements was 0.1‰ for δ¹⁸O and 0.3‰ for δD.

192 **2.4 Other data resources**

193 ~~Unique insights into the sub-permafrost environment in Adventdalen were available to our study on account of the legacy of~~
194 ~~geological exploration in the region, currently managed by the Store Norske Spitsbergen Kulkompani. This includes many~~
195 ~~unpublished borehole logs and other insights into gas accumulation beneath the permafrost in Adventdalen, which were used~~
196 ~~for the benefit of the present paper. Furthermore, deep coring, borehole investigation and geophysical surveys have also been~~

197 ~~undertaken in the same region as part of the UNIS CO₂ Project (Braathen et al, 2012; Huq et al, 2017), whose published data~~
198 ~~resources are used below to augment both our own data from the pingo springs, and unpublished data from the mining reports.~~

199 **3 Results**

200 **3.1 Sub-permafrost groundwater chemistry inferred from pingo springs**

201 Table 1 shows the geochemistry of all the water samples collected prior to the onset of snow melt from the open system pingos
202 in Adventdalen. These waters were typically brackish (Cl⁻ concentrations 390 – 1600 mg L⁻¹), largely lacking in dissolved
203 oxygen (0.00 – 2 mg L⁻¹) and NO₃⁻ (≤0.15 mg L⁻¹) and with a pH from circum-neutral to alkaline (pH 6.8 – 8.2). Figure 3A
204 shows oxidation-reduction potential (ORP) measurements, indicating that strongly reducing conditions (negative ORP) existed
205 nearest the coast (typically < -180 mV at Førstehytte and Lagoon Pingos) whilst higher, more variable values were encountered
206 up-valley (-189 to + 130 mV) at Innerhytte and River Bed Pingos.

207

208 With the exception of the River Bed Pingo Distal samples from 2017, the generally observed water type was Na-HCO₃ with a
209 saturation index (SI) for calcite indicating near-equilibrium (SI_{calcite} = 0.1 ± 0.4) according to WEB-PHREEQ. The dominance
210 of Na⁺ over the other cations (Ca²⁺, Mg²⁺ and K⁺: Table 1) and the increasing Na⁺ to Cl⁻ ratios towards the coast (Figure 3A)
211 show how cation exchange (freshening) and rock-weathering effects were increasingly influential down the valley.
212 Concentrations of SO₄²⁻ in most samples were far lower than expected when compared to late summer baseflow concentrations
213 in local rivers (e.g. Hodson et al, 2016; Rutter et al, 2011; Yde et al, 2008). However, the River Bed Pingo Distal samples
214 revealed a distinctly different spring water chemistry, with a Mg-Ca-SO₄ water type, far higher SO₄²⁻ concentrations and a
215 saturation index for gypsum that reached equilibrium (SI_{gypsum} = 0.0 ± 0.1) according to WEB-PHREEQ. Otherwise, the River
216 Bed Pingo samples from 2015 and 2016 showed sub-saturation with respect to gypsum (SI_{gypsum} = -2.9 ± 0.5). The markedly
217 different Mg-Ca-SO₄ water type therefore suggested a different groundwater source whose composition was governed by
218 gypsum-driven de-dolomitization, a process wherein very reactive gypsum catalyses the replacement of dolomite by calcite
219 (Bischoff et al, 1994). ~~However, these samples were collected a greater distance from the pingo than those in 2015 and 2016.~~
220 ~~Further field observations in 2018 and 2019 (data not shown) clearly suggest there is another groundwater source here and~~
221 ~~further east.~~ This is further supported by the different δ¹⁸O-H₂O and δD-H₂O stable isotope characteristics of the River Bed
222 Pingo Distal waters, which Figure 3B suggests were more similar to those encountered at Lagoon Pingo.

223

224 With the exception of the River Bed Pingo Distal waters, Figure 3B indicates a general westward depletion (decrease) in both
225 water isotopes towards the coast, where water samples also lie closest to the Local Meteoric Water Line (LMWL) (Rozanski
226 et al, 1993). Although Figure 4B shows that none of the waters depart significantly from the LMWL, a linear regression model

227 produces a lower slope (6.09) than that which is associated with the LMWL (i.e. 6.97), suggesting minor isotopic fractionation
228 associated with partial re-freezing (Lacelle, 2011).

229

230 **3.2 Methane geochemistry in the pingo springs**

231 Table 2 shows that concentrations of methane in pingo spring waters in both the pre-melt season and the summer periods lay
232 in the range 0.6 – 42.6 mg L⁻¹, which is up to five orders of magnitude greater than calculated atmospheric thermodynamic
233 equilibrium values, and places the most concentrated values marginally above the solubility limit for fresh water at 0 °C (i.e.
234 41 mg L⁻¹). The data include samples collected opportunistically from the springs during the summer melt season. The
235 dissolved carbon dioxide concentrations were also in excess of atmospheric equilibrium, by as much as 700 mg L⁻¹ at Innerhytte
236 Pingo. Temporal variability in the dissolved gas concentrations was significant at all sites, but greatest at River Bed Pingo
237 Distal, where there were generally much lower methane and excess CO₂ concentrations. The methane concentration (at all
238 sites) was positively correlated ($p < 0.05$) with excess CO₂ ($r = 0.86$: Figure 3C), the stable isotopes of water ($\delta^{18}\text{O-H}_2\text{O}$, $r =$
239 0.86 and $\delta\text{D-H}_2\text{O}$, $r = 0.91$: Figure 4D) and Na⁺ ($r = 0.74$).

240

241 Table 2 shows that the $\delta^{13}\text{C}$ of methane and dissolved inorganic carbon ($\delta^{13}\text{C-CH}_4$ and $\delta^{13}\text{C-DIC}$ respectively) were variable,
242 especially at Lagoon Pingo and Førstehytte Pingo. The $\delta^{13}\text{C-CH}_4$ lay between -70.7‰ and -48.2‰ VPDB, which is indicative
243 of biogenic methane at the ¹³C-depleted (more negative) end of the scale, and either partially oxidised biogenic or geogenic
244 methane at the ¹³C-enriched (more positive) upper end (Schoell, 1980). Table 2 also includes samples collected
245 opportunistically from the springs during the summer. These show that the methane concentration in summer is within the
246 range reported during late winter. The $\delta^{13}\text{C-CH}_4$ and $\delta^{13}\text{C-DIC}$ values of the summer samples are also similar to the late winter,
247 although the $\delta^{13}\text{C-CH}_4$ is marginally lower (¹³C-depleted) at Lagoon Pingo and the summer $\delta^{13}\text{C-DIC}$ values at Førstehytte
248 Pingo and Innerhytte Pingo are slightly higher (¹³C-enriched) than typical values in late winter.

249

250 Figure 4 shows that all measured $\delta^{13}\text{C-CH}_4$ values in the pingo springs compare well with the results of the pore gas extractions
251 (range – 53‰ VPDB to – 69‰ VPDB) from the upper core sections at the CO₂ Well Park (Well Site B in Figure 2: data from
252 Huq et al, 2017). Here, the methane in the permafrost and underlying host rocks of the sub-permafrost aquifer has been
253 attributed to a biogenic source because the $\delta^{13}\text{C-CH}_4$ values are moderately ¹³C-depleted (i.e. more negative) and the
254 concentrations of other hydrocarbons (propane and ethane) are low relative to methane (see Figure 4). Nearby, methane with
255 $\delta^{13}\text{C-CH}_4$ between -48.9 and -52.9‰ VPDB, and no other detectable hydrocarbons, was also found immediately beneath the
256 permafrost at Well Sites C and D in association with a Cl-rich (1500 mg L⁻¹) groundwater (Store Norske Spitsbergen
257 Kullkompani, Unpublished Report SN1983-004). In this case, both the $\delta^{13}\text{C-CH}_4$ and the Cl⁻ concentrations compare
258 favourably to the values at Innerhytte and River Bed Pingos. By contrast, the $\delta^{13}\text{C-CH}_4$ values from the pingos did not compare
259 well with the ¹³C-enriched $\delta^{13}\text{C-CH}_4$ values (range -50 ‰ to – 32 ‰ VPDB) recorded from the deeper shale unit (ie > 300 m:

260 see Figure 4) at Well Site B by Huq et al (2017). These values were assumed to indicate the deeper geogenic methane source
261 because ethane and propane were also detected at significant concentrations relative to the methane (see also Ohm et al, 2019).
262
263 Figure 4 also shows that the $\delta^{13}\text{C}$ -DIC values (range -8.5‰ to +26‰ VPDB) observed in the pingo springs do not compare
264 well with the values from the lower shale-rich units of the rock cores either (range -26‰ to +21‰ vPDB: Huq et al, 2017).
265 This difference cannot be attributed to differences in the DIC speciation among our water samples (containing $\text{CO}_{2(\text{aq})}$, H_2CO_3 ,
266 HCO_3^- and CO_3^{2-}) and the published rock pore gas samples ($\text{CO}_{2(\text{g})}$ only). The low $\delta^{13}\text{C}$ -DIC that is missing from the pingo
267 water samples derives from organic matter respiration and is known to be present in local riverine runoff ($\delta^{13}\text{C}$ -DIC range -
268 15‰ to -4‰ VPDB: Hindshaw et al, 2016). Therefore, the higher $\delta^{13}\text{C}$ -DIC signatures of the pingo springs are most similar
269 to those seen in the upper aquifer zone of the cores, and for $\delta^{13}\text{C}$ -DIC in excess of +10‰ VPDB, may be attributed to the
270 carbon isotope fractionation during the reduction of CO_2 to CH_4 during hydrogenotrophic methanogenesis (Huq et al, 2017;
271 Schoell, 1980).

272 4 Discussion

273 4.1 Groundwater geochemical environment and methane concentrations

274 The geochemistry of the pingo springs is significantly different to surface waters in the Adventdalen watershed (see Hodson
275 et al, 2016; Rutter et al, 2011; Yde et al, 2008). Their high Cl^- concentrations and distinct Na-HCO_3 freshening signature
276 indicate flushing-incorporation of brackish-marine pore-water from either the uplifted, Holocene marine sediments, the fjord,
277 or a mixture of the two. Importantly, the removal of nitrate and sulphate and the presence of biogenic methane indicate that
278 microbially-mediated processes operate (denitrification, sulfate reduction and methanogenesis, respectively). These decrease
279 the redox potential of the groundwaters towards the low ORP conditions found at the coast (Figure 3a). The strikingly different
280 water chemistry dominated by Mg-Ca- SO_4 in the River Bed Pingo Distal samples during 2017 seems to indicate an additional
281 ground water type that is strongly influenced by the gypsum- and dolomite-bearing rocks that outcrop east of Adventdalen, or
282 lie at considerable depth (beneath the Agardfjellet Formation) within the study area in Figure 2. Due to the low hydraulic
283 conductivity of the shale units of the Rurikfjellet and Agardfjellet Formations, their influence upon springs at the River Bed
284 Pingo Distal site is presumably made possible by groundwater migration along the faults in the vicinity of pingo (Figure 2a).
285 Otherwise, sub-permafrost groundwater migration in the study area seems dominated by the exploitation of the sub-permafrost
286 aquifer hosted by the Helvetiafjellet Formation in the lower valley (see Hornum et al, In Review).

287
288 The strongest predictors of the methane content in the pingo springs are $\delta^{18}\text{O}$ - H_2O and δD - H_2O (Figure 3d). Since the $\delta^{18}\text{O}$ -
289 H_2O and δD - H_2O show only a minor departure from the LMWL (Figure 3b), this indicates a strong water source control upon
290 the gas concentration emerging from the pingos. Methane concentrations generally increase up-valley where $\delta^{18}\text{O}$ - H_2O and
291 δD - H_2O become more ^{18}O -enriched. Since sea water is $\delta^{18}\text{O}$ - and δD -enriched relative to freshwater, the simplest, although

292 initially counter-intuitive explanation for this change, is an inland increase in the mixing ratio of marine ~~po~~re-waters within
293 the sub-permafrost groundwater. A statistically significant ($p < 0.05$) relationship between Cl^- and methane ($r = 0.74$) also
294 becomes apparent when the River Bed Pingo Distal samples are excluded. The dependence of the methane concentration upon
295 Cl^- , $\delta^{18}\text{O}\text{-H}_2\text{O}$ and $\delta\text{D}\text{-H}_2\text{O}$ is therefore consistent with deeper, denser sub-permafrost brines providing the water source to the
296 pingo springs further inland. Hornum et al (In Review) show how this most likely reflects a general increase in the thickness
297 of the permafrost with distance from the coast (shown crudely in Figure 1b). The presence of the Mg-Ca-SO₄ groundwater in
298 the River Bed Pingo Distal samples is also consistent with this interpretation, because the gypsum-hosting Permian strata lie
299 beneath the Agardfjellet Formation. Further down-valley, where permafrost is thinner, a greater mixing ratio of fresher, low
300 density groundwater discharges from the pingo springs. Its more depleted (lower) $\delta^{18}\text{O}\text{-H}_2\text{O}$ and $\delta\text{D}\text{-H}_2\text{O}$ signature is consistent
301 with dilution by snow and ice melt from the mountains that flank the main valley axis near the coast (Yde et al, 2008).

302 4.2 Methane sources and removal

303 Comparison of the pingo $\delta^{13}\text{C}\text{-CH}_4$ to the rock core gas samples in Figure 4 shows that mixtures of biogenic methane (lower
304 $\delta^{13}\text{C}\text{-CH}_4$ signatures) and geogenic methane (higher $\delta^{13}\text{C}\text{-CH}_4$ signatures) might be present beneath the permafrost. However,
305 evidence for a significant geogenic methane contribution to the pingo springs is equivocal and seems unlikely given the low
306 rates of fluid migration that may be expected in the deeper shale-rich Rurikfjellet and Agardfjellet Formations. Therefore, the
307 partial oxidation of biogenic methane most likely explains the occasionally higher $\delta^{13}\text{C}\text{-CH}_4$ signatures in the pingo springs,
308 due to the preferential oxidation of the ^{12}C isotopes (leaving the residual pool ^{13}C enriched: Schoell, 1980). The most variable
309 $\delta^{13}\text{C}\text{-CH}_4$ values were encountered at Førstehytte and Lagoon Pingos (mean ± 1 standard deviation: $-58.8 \pm 7.11\%$ VPDB and
310 $-62.2 \pm 8.81\%$ VPDB, respectively) and include the only low $\delta^{13}\text{C}\text{-CH}_4$ values which can be attributed to biogenic methane
311 with reasonable certainty (Table 2). Significant variations in these $\delta^{13}\text{C}\text{-CH}_4$ values sometimes occurred relatively rapidly, for
312 example from -55.3 to -67.4% VPDB in just nine days at Førstehytte Pingo (April 2016), or from -62.0 to -48.3 to -55.6%
313 VPDB over 34 days at Lagoon Pingo (March to April 2017). Rather than invoking an unlikely, rapid switching between
314 geogenic ($\delta^{13}\text{C}\text{-CH}_4$ -enriched) and a biogenic ($\delta^{13}\text{C}\text{-CH}_4$ -depleted) methane sources, it is far more plausible that this variability
315 was caused by changing degrees of oxidation of biogenic methane during storage beneath the surface ice blisters at the pingos.
316 We therefore contend that as storage beneath an ice lid proceeds, the $\delta^{13}\text{C}\text{-CH}_4$ at these sites will become increasingly $\delta^{13}\text{C}\text{-}$
317 CH₄-enriched until hydraulic or thermal fracturing allows the trapped fluids to escape. Methanotrophic microbial communities
318 in the marine muds represent a plausible mechanism for the enrichment (Hodson et al, 2019). After an outburst event,
319 refreezing then seals the system and the void fills once more with $\delta^{13}\text{C}\text{-CH}_4$ -depleted, biogenic methane. As a consequence,
320 the time elapsed since the last fracture event, as well as the volume fraction of the fluids that managed to escape before
321 refreezing, are both likely to cause the notable variations in the $\delta^{13}\text{C}\text{-CH}_4$ of our samples. For this reason, Table 2 shows that
322 samples collected opportunistically at these sites during late summer (when no ice lid existed) consistently showed the depleted
323 $\delta^{13}\text{C}\text{-CH}_4$ values (i.e. between -60 and -70% VPDB) expected of a biogenic source.

324

325 The high methane concentrations at Innerhytte Pingo, sometimes observed near the solubility limit (ca. 41 mg L⁻¹), were
326 characterised by limited variability in $\delta^{13}\text{C-CH}_4$ (mean $\leftarrow -54.4 \pm 2.82\%$ VPDB). The $\delta^{13}\text{C-CH}_4$ values at nearby River Bed
327 Pingo ($-54.5 \pm 1.76\%$ VPDB) were almost identical, and again showed far less variability than at Førstehytte and Lagoon
328 Pingos. If the high concentrations and invariable $\delta^{13}\text{C-CH}_4$ are indicative of minimal removal or carbon isotope fractionation
329 beneath an ice lid, then these results reveal a different (more ¹³C-enriched) $\delta^{13}\text{C-CH}_4$ source signature than at Lagoon Pingo
330 and Førstehytte Pingo. A mixture of geogenic and biogenic gas therefore seems more plausible here, not least because the
331 $\delta^{13}\text{C-CH}_4$ signatures lie close to the geogenic methane $\delta^{13}\text{C-CH}_4$ signature inferred from the lower shale units by Huq et al
332 (2017) (i.e. $\delta^{13}\text{C-CH}_4$ ca. -45% VPDB and above: Figure 4). However, the $\delta^{13}\text{C-CH}_4$ signatures are in fact closest to the gas
333 discovered in the Helvetiafjellet aquifer just below the permafrost at Wells C and D (i.e. $\delta^{13}\text{C-CH}_4$ between -48.9 and -52.9%
334 VPDB), which is known to be almost entirely biogenic because there are low or undetectable levels of other hydrocarbons
335 (ethane and propane) according to both SNSK reports and Huq et al (2017). Furthermore, the high $\delta^{13}\text{C-DIC}$ ($> 10\%$) at both
336 Innerhytte and River Bed Pingos, also observed in the sub-permafrost aquifer by Huq et al (2017), are strongly indicative of
337 CO₂ reduction by the hydrogenotrophic pathway of biogenic methanogenesis (Schoell, 1980). Therefore, the partial oxidation
338 of biogenic methane also provides the simplest explanation for the presence of this gas at high concentrations in pingo outflows
339 further up-valley.

340

341 **4.3 Pingos and springs as methane emission hotspots**

342 In spite of there being evidence for sub-surface oxidation and/or methanotrophy in our winter samples, our data clearly show
343 that others reach, or even marginally exceed, the methane solubility limit (i.e. 41 mg L⁻¹ in freshwater at 0 °C) prior to their
344 discharge from the pingo. The potential contribution of the pingos to the annual land-to-atmosphere methane flux therefore
345 deserves appraisal. We address this by first showing that the flux of methane transported to the land surface is significant
346 compared to known wetland methane emissions in our study area. Then we describe how removal processes immediately after
347 the spring waters discharge from the pingos are far less effective than is known to be the case with submarine emissions in the
348 Svalbard region (Mau et al. 2017).

349

350 The flux of methane transported to the land surface was estimated from the product of the pingo outflow rates (water discharge)
351 and their average methane concentration. The water discharge was assumed constant at each site, on account of the likelihood
352 of prolonged residence time beneath the permafrost, our own visual inspection of the flows throughout the study, and the fact
353 that discharge is largely driven by the gradual process of permafrost aggradation in response to isostatic uplift (Hornum et al.
354 2019; Yoshikawa and Harada, 1995). Our flow observations include monitoring that was undertaken at Lagoon Pingo, which
355 demonstrated little seasonal variation in groundwater flow (Hodson et al. 2019). Published values of the pingo spring
356 discharges are scarce, but range from 0.01 to 3 L s⁻¹ (Hodson et al. 2019; Hornum et al. In Review; Liestøl, 1996; Yoshikawa,
357 1993). The flows used for each site are described in Table 3 and amount to a combined discharge of ca. 1.6 L s⁻¹. In addition

358 to the four pingo springs, a large spring discharge (measured at 0.52 L s⁻¹ in October 2018) at a site 100 m west of Lagoon
359 Pingo has been included after it was discovered to contain high methane concentrations. The average methane concentration
360 of this site “Lagoon Pool” was 22.2 ± 1.9 mg L⁻¹ (n = 4) according to samples taken through an ice cover in February, March
361 and October, 2018. At these times, the electrical conductivity was very similar to the outflow at Lagoon Pingo and it was
362 inferred to be the same water source.

363

364 Table 3 shows that the total methane flux from the pingo springs is ca. 1051 kg CH₄ y⁻¹. For comparison, rates of methane
365 emission from chambers installed over the course of three years in an ice wedge polygon site in Adventdalen lie in the range
366 0 – 5 gC m⁻² yr⁻¹ according to Pirk et al (2017), with a median of ca. 1 gC m⁻² yr⁻¹. Assuming that all other wetlands in the
367 valley floor contributed equally (from an area of 4.7 km²), the total active layer emissions were probably between 6040 and
368 10400 kg CH₄ yr⁻¹. Our estimates of pingo spring methane fluxes are therefore equivalent to up to 17% of the active layer
369 emissions.

370

371 The magnitude of annual methane emission from the springs to the atmosphere very much depends upon the hydrological and
372 meteorological conditions at each pingo site, as well as their variation during the year. During winter, all the sites were
373 characterised by a large ice blister, from which periodic outbursts of methane-rich water occurred. During these outbursts,
374 methane emission is most efficient on account of the flow turbulence and likely rejection of methane from the icing formed by
375 the runoff as it gradually freezes (usually within 100 m of the outburst source). Measurement of the methane evasion from the
376 outburst was impossible under winter conditions, although it was possible to capture the rapid, downstream loss of dissolved
377 methane using samples taken opportunistically during an outburst event on 22nd April 2015. Figure 5 shows how the
378 downstream methane concentration decreased with distance from the pingo icing summit in a manner described by a regression
379 model of the form:

$$380 \quad \text{_____} (CH_{4(aq)})_x = 16.9X^{-0.384} \quad \text{_____} \text{Eq. 1)$$

381 Where (CH_{4(aq)})_x is the dissolved methane concentration at distance X (m) from the pingo icing summit. The coefficient of
382 determination was 0.90 (n = 6) using only the 2015 data. Other samples from the base of the pingo in 2014 are used to show
383 how methane concentrations at greater distances away from the pingo are far lower and thus consistent with further methane
384 loss (see Table 2). The rapid loss of methane was not well accounted for by an exponential model, which yielded a coefficient
385 of determination of 0.70 (not shown). Although this outcome is highly sensitive to the single data point at 3 m from the icing
386 summit, it most likely implies that turbulence was non-linear along the flow path and greatly enhanced the rate of methane
387 evasion as the spring descended the steep, initial part of the pingo flank. Freezing effects were not discernible in the 2015
388 transect until after the spring flowed onto the flat valley floor (ie beyond 50 m in Figure 5), where the flow velocities decreased
389 markedly. With this being the case, the data show that 94 % of the methane was most likely lost to the atmosphere within 44
390 m of the inferred spring source. During winter, turbulence-driven gas exchange therefore seems most effective near the pingo
391 summit, whilst freezing effects dominate once springs have flowed onto the valley floor (but add little to the overall flux).

392

393 During summer, significant changes at the surface of the pingos means that two key emission scenarios require consideration:
394 i) a low emission scenario, caused by springs discharging straight into a receiving water body, such as a pool (Lagoon Pingo
395 and Lagoon Pool) or the river (River Bed Pingo), and ii) a higher emission scenario caused by turbulent discharge down the
396 flank of the pingo (Førstehytte Pingo and Innerhytte Pingo) and therefore similar to the winter emission scenario but with less
397 freezing effects. Hodson et al (2019) examined the first scenario at Lagoon Pingo and showed that the pond which forms above
398 the groundwater spring during summer reduces the annual emission flux to 42 kg CH₄ y⁻¹, which is 0.65 times the spring
399 discharge flux according to Table 3. This reduction was caused by inundation of the site by meltwater (including that derived
400 from ablation of the ice lid) and rainfall. We presume a similar reduction occurs every summer at River Bed Pingo Site, where
401 a large river engulfs the entire spring. However, the pond that forms above Lagoon Pingo does not form every year due to the
402 susceptibility of the drainage pathway at this site to the disturbance caused by its ice lid collapse. Therefore, by 2020, the
403 system had reverted to a single spring discharging from a point source, rather like the situation at Innerhytte Pingo. Interannual
404 variations in atmospheric methane emissions from pingos are therefore very likely.

405

406 The discovery of methane-rich sub-permafrost groundwaters discharging from Svalbard's open system pingos means that other
407 perennial springs also deserve attention, because they may be carrying the same fluids. Modelling studies also imply that an
408 increase in the discharge of groundwater systems into surface hydrological networks can be expected as climate change
409 proceeds (Bense et al, 2012). Since these perennial springs result in the formation of winter icings similar to those encountered
410 on the summit or flanks of the pingos, their detection is greatly facilitated. As a consequence, it is well known in Svalbard that
411 they constitute groundwater flows greatly in excess of those observed flowing from pingos (Bukowska-Jania and Szafraniec,
412 2005). The sensitivity of the total atmospheric methane flux caused by the ventilation of sub-permafrost groundwater discharge
413 is therefore potentially very important. For example, a total discharge of sub-permafrost groundwaters of just 50 L s⁻¹ with a
414 methane concentration of 17.9 mg L⁻¹ (i.e. average of all values in Table 2) would mean more than five times more methane
415 is available for emission from the land surface to the atmosphere (if active layer emissions remain constant). Such a
416 groundwater discharge would still only represent 0.001% of the total annual runoff in Adventdalen during the study (A. Nowak
417 and A. Hodson, Unpublished Data). Evidence for similar coastal groundwater springs with high methane concentrations that
418 contribute meaningfully to emission fluxes exist elsewhere in the Arctic, including the MacKenzie Delta, Alaska, where they
419 are thought to contribute approximately 17% of the emission from the delta (Kohnert et al, 2017). All forms of sub-permafrost
420 groundwater discharge in Arctic coastal lowlands therefore deserve closer attention in order to better understand changes in
421 the release of sub-permafrost methane to the atmosphere.

422

423 5 Conclusion

424 The development of open system pingos in Svalbard's coastal lowlands is linked to permafrost aggradation following isostatic
425 uplift. This mechanism results in the expulsion of methane-rich sub-permafrost fluids over the course of centuries at individual
426 sites, and establishes pingos as potential hotspots for greenhouse gas emissions. In Central Spitsbergen, the concentrations of
427 methane in the springs that discharge from open system pingos are high (flow weighted average 17.9 mg L^{-1} , and can even
428 marginally exceed the solubility limit of ca. 41 mg L^{-1}). The methane appears to be largely biogenic in origin and subject to
429 moderate levels of oxidation. However a geogenic methane origin cannot be ruled out because it is present at greater depths
430 beneath the permafrost. The methane is brought to the surface of Adventdalen after groundwaters have exploited faults through
431 mudstones of low hydraulic conductivity to the east, and sandstones of high hydraulic conductivity to the west. The study of
432 open system pingos therefore offers rare insights into sub-permafrost methane and groundwater dynamics. Since this is one of
433 the least understood potential emission sources, open system pingos deserve greater research attention, so that sub-permafrost
434 emission sources can be integrated with those from the active layer for better emission forecasts. In our study, ca. 1051 kg CH_4
435 yr^{-1} was transported to the land surface at~~released from just~~ four pingos with a trivial combined groundwater discharge of ca.
436 1.6 L s^{-1} . The high gas concentrations in the pingo springs that is responsible for this potentially significant emission shows
437 that all types of sub-permafrost groundwater spring, however small, deserve appraisal as methane emission sources.

438

439 6 Data Availability

440 Detailed water quality parameters, including methane concentrations and isotopic composition, for groundwater springs
441 discharging from open system pingos in Adventdalen, Svalbard (2015-2017) are available at
442 <https://doi.org/10.5285/3D82FD3F-884B-47B6-B11C-6C96D66B950D>.

443

444 Author Contributions

445 AJH, AN, PB and MTH collected the samples and analysed the data, with significant input from SJ, KR and AVT. The
446 laboratory samples were analysed by SFT, AJH, KR and AVT. AJH wrote the manuscript, with equal editorial input from the
447 remaining authors.

448

449 Competing financial interests

450 The authors declare no competing financial interests.

452 **Acknowledgements**

453 The authors acknowledge Joint Programming Initiative (JPI-Climate Topic 2: Russian Arctic and Boreal Systems) Award No.
454 71126, UK Natural Environment Research Council grant NE/M019829/1, UK Natural Strategic Environment Science Capital
455 Funding, Research Council of Norway grants (NRC nos. 244906 and 294764) and a Royal Geographical Society Ralph Brown
456 Expedition Award 2017. Andrew Fairburn (University of Sheffield) and Stephen Reid (University of Leeds) are thanked for
457 performing the dissolved gas and chemical analysis of the water samples.

458

459 **References**

460 Anthony, K. M. W., Anthony, P., Grosse, G. & Chanton, J. Geologic methane seeps along boundaries of Arctic permafrost
461 thaw and melting glaciers, *Nat. Geosci.*, 5(6), 419-426, 2012.

462 Bense, V. F., Kooi, H., Ferguson, G. and Read, T.: Permafrost degradation as a control on hydrogeological regime shifts in a
463 warming climate, *J. Geophys. Res. Earth Surf.*, 117(3), 1–18, doi:10.1029/2011JF002143, 2012.

464 Bergman, T. L., Lavine, A. S., Incropera, F. P. and Dewitt, D. P.: *Fundamentals of Heat and Mass Transfer*. 7th Edition, ,
465 1048, doi:10.1007/s13398-014-0173-7.2, 2011.

466 Betlem, P., Senger, K., and Hodson, A.: 3D thermobaric modelling of the gas hydrate stability zone onshore central
467 Spitsbergen, Arctic Norway, *Marine and Petroleum Geology*, 100, 246-262, 2019.

468 Bischoff, J. L., Juliá, R., Shanks III, W. C. and Rosenbauer, R. J.: Karstification without carbonic acid: Bedrock dissolution
469 by gypsum-driven dedolomitization, *Geology*, 22(11), 95-998, 1994.

470 Braathen, A., Bælum, K., Christiansen, H. H., Dahl, T., Eiken, O., Elvebakk, H., Hansen, F., Hanssen, T. H., Jochmann, M.,
471 Johansen, T. A., Johnsen, H., Larsen, L., Lie, T., Mertes, J., Mørk, A., Mørk, M. B., Nemeč, W. J., Olaussen, S., Oye, V., Rød,
472 K., Titlestad, G. O., Tveranger, J. & Vagle, K. Longyearbyen CO₂ lab of Svalbard, Norway – first assessment of the
473 sedimentary succession for CO₂ storage, *Norwegian Journal of Geology*, 92, 353–376, 2012.

474 Bukowska-Jania, E., and Szafraniec, J.: Distribution and morphometric characteristics of icing fields in Svalbard, *Polar*
475 *Res.*, 24(1-2), 41-53, 2005.

476 Cable, S., Elberling, B. and Kroon, A.: Holocene permafrost history and cryostratigraphy in the High-Arctic Adventdalen
477 Valley, central Svalbard, *Boreas*, 47(2), 423-442, 2018.

478 Crémière, A., Lepland, A., Chand, S., Sahy, D., Condon, D.J., Noble, S. R., Martma, T., Thorsnes, T., Sauer, S. and Brunstad,
479 H.: Timescales of methane seepage on the Norwegian margin following collapse of the Scandinavian Ice Sheet, *Nat. Comms.*,
480 7, 11509, 2016.

481 Dean, J. F., Middelburg, J. J., Röckmann, T., Aerts, R., Blauw, L. G., Egger, M., Jetten, M. S., de Jong, A. E., Meisel, O. H.,
482 Rasigraf, O. and Slomp, C.P.: Methane feedbacks to the global climate system in a warmer world, *Rev. Geophys.*, 56(1), 207-
483 250, 2018.

484 Dmitrenko, I. A., Kirillov, S. A., Tremblay, L. B., Kassens, H., Anisimov, O. A., Lavrov, S. A., Razumov, S. O. and Grigoriev,
485 M. N.: Recent changes in shelf hydrography in the Siberian Arctic: Potential for subsea permafrost instability, *J. Geophys.*
486 *Res.: Oceans*, 116, C10, 2011.

487 Dutton, A., Carlson, A. E., Long, A. J., Milne, G.A., Clark, P. U., DeConto, R., Horton, B. P., Rahmstorf, S. and Raymo, M.
488 E.: Sea-level rise due to polar ice-sheet mass loss during past warm periods, *Science*, 349, 6244, 2015.

489 Frederick, J. M. and Buffett, B. A.: Submarine groundwater discharge as a possible formation mechanism for permafrost-
490 associated gas hydrate on the circum-Arctic continental shelf, *J. Geophys. Res.: Earth*, 121(3), 1383-1404, 2016.

491 Gautier, D. L., Bird, K. J., Charpentier, R. R., Grantz, A., Houseknecht, D. W., Klett, T. R., Moore, T. E., Pitman, J. K.,
492 Schenk, C. J., Schuenemeyer, J. H. and Sørensen, K.: Assessment of undiscovered oil and gas in the Arctic. *Science*, 324(5931),
493 1175-1179, 2009.

494 Gilbert, G. L., Cable, S., Thiel, C., Christiansen, H. H. and Elberling, B.: Cryostratigraphy, sedimentology, and the late
495 Quaternary evolution of the Zackenberg River delta, northeast Greenland, *The Cryosphere*, 11(3), 1265, 2017.

496 Gilbert, G. L., O'Neill, H. B., Nemeč, W., Thiel, C., Christiansen, H. H., and Buylaert, J.P.: Late Quaternary sedimentation
497 and permafrost development in a Svalbard fjord-valley, Norwegian high Arctic, *Sedimentology*, 65, 2531–2558, 2018.

498 Hindshaw, R.S., Lang, S.Q., Bernasconi, S.M., Heaton, T.H.E., Lindsay, M.R. and Boyd, E.S.: Origin and temporal variability
499 of unusually low $\delta^{13}\text{C}$ -DOC values in two High Arctic catchments. *J. Geophys. Res.: Biogeo.*, 121(4), 1073-1085 (2016).

500 Hodson, A., Nowak, A. and Christiansen, H.H.: Glacial and periglacial floodplain sediments regulate hydrologic transfer of
501 reactive iron to a high arctic fjord, *Hydrol. Proc.*, 30(8), 1219-1229, 2016.

502 Hodson, A. J., Nowak, A., Holmlund, E., Redeker, K. R., Turchyn, A. V., & Christiansen, H. H.: Seasonal dynamics of
503 Methane and Carbon Dioxide evasion from an open system pingo: Lagoon Pingo, Svalbard, *Frontiers in Earth Science*, 7, 30,
504 2019.

505 [Hornum, M. T., Hodson, A. J., Jessen, S., Bense, V., and Senger, K.: Numerical modelling of permafrost spring discharge and](#)
506 [open-system pingo formation induced by basal permafrost aggradation, *The Cryosphere Discuss.*, \[https://doi.org/10.5194/tc-\]\(https://doi.org/10.5194/tc-2020-7\)](#)
507 [2020-7, in review, 2020.](#)

508 Huq, F., Smalley, P. C., Mørkved, P. T., Johansen, I., Yarushina, V. & Johansen, H.: The Longyearbyen CO₂ Lab: Fluid
509 communication in reservoir and caprock, *Int. J. Greenhouse Gas Control*, 63, 59-76, 2017.

510 Keating, K., Binley, A., Bense, V., Van Dam, R. L., and Christiansen, H. H.: Combined geophysical measurements provide
511 evidence for unfrozen water in permafrost in the Adventdalen valley in Svalbard, *Geophys. Res. Lett.*, 45(15), 7606-7614,
512 2018.

513 Kohnert, K., Serafimovich, A., Metzger, S., Hartmann, J., and Sachs, T.: Strong geologic methane emissions from
514 discontinuous terrestrial permafrost in the Mackenzie Delta, Canada, *Scientific Reports*, 7(1), 5828, 2017.

515 Lacelle, D.: On the $\delta^{18}\text{O}$, δD and D-excess relations in meteoric precipitation and during equilibrium freezing: theoretical
516 approach and field examples, *Permafrost Periglac.*, 22(1), 13-25, 2011.

517 Liestøl, O.: Open System pingos in Spitsbergen, *Norsk Geogr. Tidsskr.*, 50(1), 81 – 84, 1996.

518 Liestøl, O.: Pingos, Springs, and Permafrost in Spitsbergen, *Årbok 1975. Norsk Polarinstitut, Tromsø, Norway*, 1977.

519 Liira, M., Noormets, R., Sepp, H., Kekišev, O., Maddison, M., and Olaussen, S.: Sediment geochemical study of hydrocarbon
520 seeps in Isfjorden and Mohnbukta: a comparison between western and eastern Spitsbergen, Svalbard, *Arktos*, 5(1), 49 – 62,
521 2019.

522 Magen, C., Lapham, L.L., Pohlman, J.W., Marshall, K., Bosman, S., Casso, M. and Chanton, J.P.: A simple headspace
523 equilibration method for measuring dissolved methane, *Limnol. Oceanogr. Methods*, 12, 637-650, 2014.

524 Mau, S., Römer, M., Torres, M.E., Bussmann, I., Pape, T., Damm, E., Geprägs, P., Wintersteller, P., Hsu, C.W., Loher, M.
525 and Bohrmann, G.: Widespread methane seepage along the continental margin off Svalbard-from Bjørnøya to Kongsfjorden,
526 *Scientific reports*, 7, 42997, 2017.

527 McAuliffe, C.: Gas Chromatographic determination of solutes by multiple phase equilibrium, *Chem. Technol.*, 1, 46-51, 1971

528 [Ohm, S. E., Larsen, L., Olaussen, S., Senger, K., Birchall, T., Demchuk, T., Hodson, A., Johansen, I., Titlestad, G. O., Karlsen,](#)
529 [D. A. and Braathen, A.: Discovery of shale gas in organic rich Jurassic successions, Adventdalen, Central Spitsbergen, Norway,](#)
530 [Norwegian Journal of Geology, 99\(2\), 349 - 276, 2019.](#)

531 [Olaussen, S., Senger, K., Braathen, A., Grundvåg, S. A. and Mørk, A.: You learn as long as you drill; research synthesis from](#)
532 [the Longyearbyen CO₂ Laboratory, Svalbard, Norway, Norwegian Journal of Geology, 99\(2\), 157 - 181, 2019.](#)

533 Pirk, N., Mastepanov, M., López-Blanco, E., Christensen, L. H., Christiansen, H. H., Hansen, B. U., Lund, M., Parmentier, F-
534 J., Skov, K. and Christensen, T. R.: Toward a statistical description of methane emissions from arctic wetlands, *Ambio*, 46(1),
535 70-80, 2017.

536 Pohlman, J. W., Greinert, J., Ruppel, C., Silyakova, A., Vielstädte, L., Casso, M., Mienert, J. and Bünz, S.: Enhanced CO₂
537 uptake at a shallow Arctic Ocean seep field overwhelms the positive warming potential of emitted methane, *Proc. Natl. Acad.*
538 *Sci. U.S.A.*, 114(21), 5355-5360, 2017.

539 Portnov, A., Vadakkepuliambatta, S., Mienert, J. and Hubbard, A.: Ice-sheet-driven methane storage and release in the Arctic,
540 *Nat. Comms.*, 7, 10314, 2016.

541 Roy, S., Senger, K., Hovland, M., Römer, M. and Braathen, A.: Geological controls on shallow gas distribution and seafloor
542 seepage in an Arctic fjord of Spitsbergen, Norway, *Marine and Petroleum Geology*, 107, 237-254, 2019.

543 Rozanski, K., Araguás-Araguás, L., and Gonfiantini, R.: Isotopic patterns in modern global precipitation, in: *Climate change*
544 *in Continental Isotopic Records* (eds. P. K. Swart, K. C. Lohmann, J. McKenzie, and S. Savin), 1–37, *Geophysical Monograph*
545 *No. 78*, American Geophysical Union, Washington D.C.1-36, 1993.

546 Rutter, N., Hodson, A., Irvine-Fynn, T. & Solås, M. K. Hydrology and hydrochemistry of a deglaciating high-Arctic catchment,
547 *Svalbard. J. Hydrol.*, 410(1), 39-50, 2011.

548 Schoell, M.: The hydrogen and carbon isotopic composition of methane from natural gases of various origins, *Geochim.*
549 *Cosmochim. Acta*, 44(5), 649–661, 1980.

550 Schuur, E. A. G., McGuire, A. D., Schädel, C., Grosse, G., Harden, J. W., Hayes, D. J., Hugelius, G., Koven, C. D., Kuhry,
551 P., Lawrence, D. M. and Natali, S. M.: Climate change and the permafrost carbon feedback, *Nature*, 520 (7546), 171-179,
552 2015.

553 Smith, L. M., Sachs, J.P., Jennings, A. E., Anderson, D. M. & DeVernal, A.: Light $\delta^{13}\text{C}$ events during deglaciation of the East
554 Greenland continental shelf attributed to methane release from gas hydrates, *Geophys. Res. Lett.*, 28(11), 2217-2220, 2001.

555 Smith, R. W., Bianchi, T. S., Allison, M., Savage, C. and Galy, V.: High rates of organic carbon burial in fjord sediments
556 globally, *Nat. Geosci.*, 8(6), 450-453, 2015.

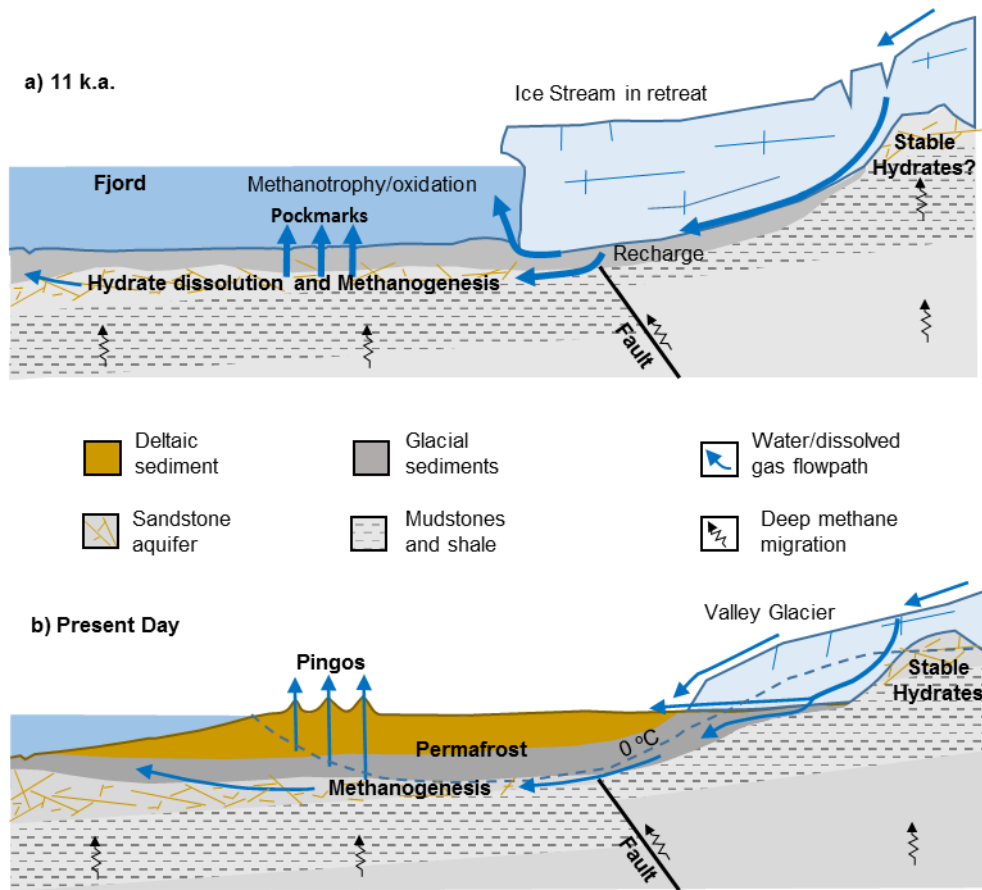
557 Syvitski, J. P. M., Burrell, D. C. and Skei, J. M.: *Fjords: Processes and Products*, Springer, New York, 377 pp, 1986.

558 Tyler, S. C., Bilek, R. S., Sass, R. L. and Fisher, F. M.: Methane oxidation and pathways of production in a Texas paddy field
559 deduced from measurements of flux, $\delta^{13}\text{C}$, and δD of CH₄, *Global Biogeochem Cycles*, 11 (3) 323-348, 1997.

560 Weitemeyer, K. A. and Buffett, B. A.: Accumulation and release of methane from clathrates below the Laurentide and
561 Cordilleran ice sheets, *Glob. Planet. Change*, 53(3), 176-187, 2006.

562 Włodarska-Kowalczyk, M., Mazurkiewicz, M., Górska, B., Michel, L.N., Jankowska, E. and Zaborska, A.: Organic carbon
563 origin, benthic faunal consumption and burial in sediments of northern Atlantic and Arctic fjords (60-81 0N), *J. Geophys. Res.:*
564 *Biogeo.*, *In Press*, doi:10.1029/2019JG005140

- 565 Yde, J. C., Riger-Kusk, M., Christiansen, H. H., Knudsen, N. T., and Humlum, O.: Hydrochemical characteristics of bulk
566 meltwater from an entire ablation season, Longyearbreen, Svalbard, *J. Glaciol.*, 54(185), 259-272 (2008).
- 567 Yoshikawa, K.: Notes on open-system pingo ice, Adventdalen, Spitsbergen, *Permafrost Periglac.*, 4, 327-334, 1993.
- 568 Yoshikawa, K. and Harada, K. Observations on nearshore pingo growth, Adventdalen, Spitsbergen, *Permafrost Periglac.*, 6(4),
569 361-372, 1995.
- 570 Yoshikawa, K., and Nakamura, T.: Pingos growth age in the delta area, Adventdalen Spitsbergen, *Polar Rec.*, 32, 347-352,
571 1996.
- 572



573

574 **Figure 1.** Landscape change and likely methane migration pathways in Adventdalen (thickness of geological units and
 575 sediments not to scale): a) during deglaciation after the Last Glacial Maximum ca. 11 000 years ago, b) today, following delta
 576 progradation, isostatic uplift and permafrost aggradation. The conceptual model of landscape change was based upon Gilbert
 577 et al (2018).

578

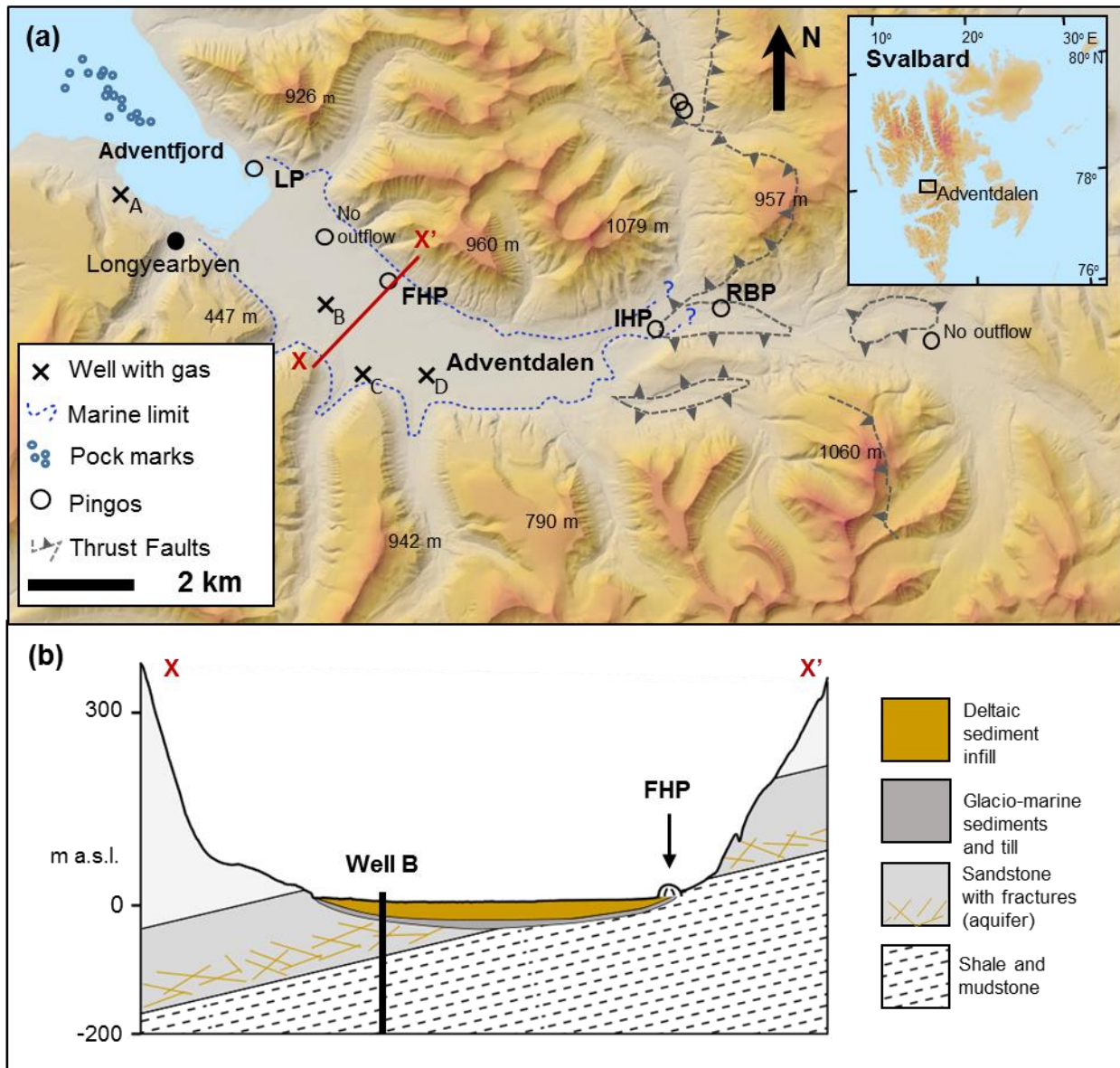
579

580

581

582

583



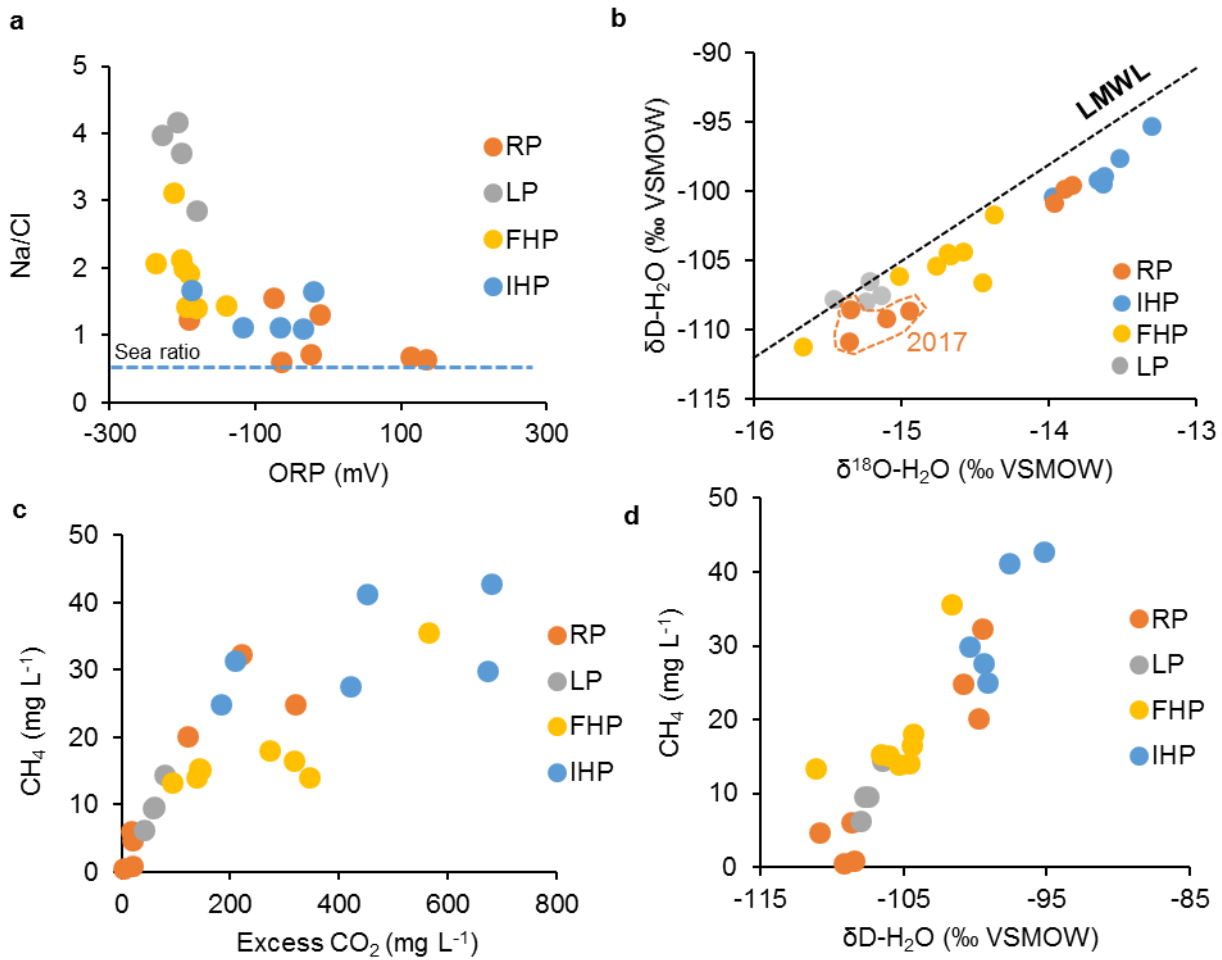
584

585

586 **Figure 2.** Adventdalen topography, pingos and geology. Active springs exist at Lagoon Pingo, Førstehytte Pingo, Innerhytte
 587 Pingo and River Bed Pingo (LP, FHP, IHP and RBP respectively). Well Sites A and B are part of the UNIS CO₂ Well Park
 588 (Braathen et al, 2012), whilst Well Sites C and D are part of the Store Norske Spitsbergen Kulkompani (SNSK) operations.
 589 Map developed online at www.svalbardkartet.npolar.no.

590

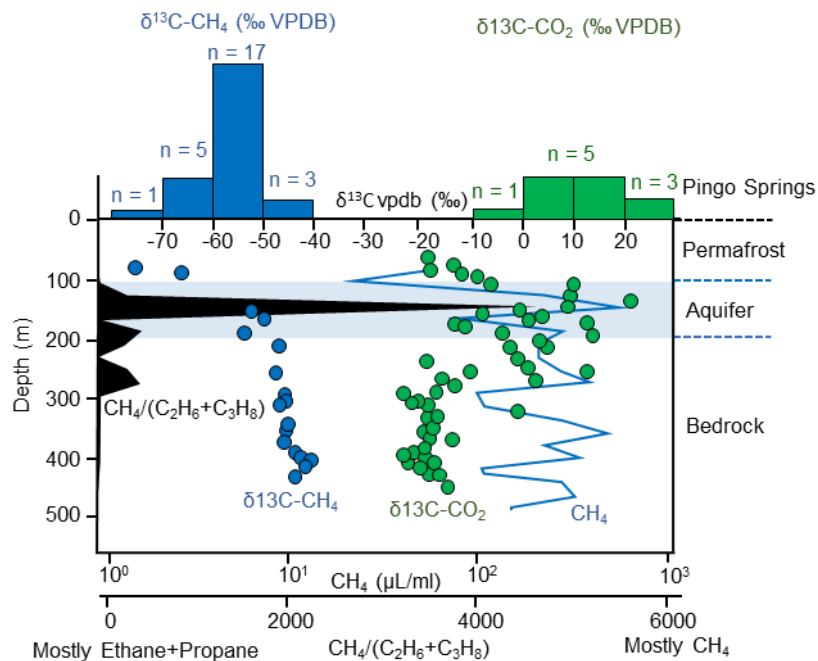
591



592
 593 **Figure 3.** Key geochemical and dissolved gas characteristics in spring waters draining River Bed Pingo (RP), Innerhytte
 594 Pingo (IHP), Førstehytte Pingo (FHP) and Lagoon Pingo (LP). “LMWL” denotes the Local Mean Water Line. The legend in
 595 Figure 3a applies also to Figures 3b – 3d.

596

597



598

599

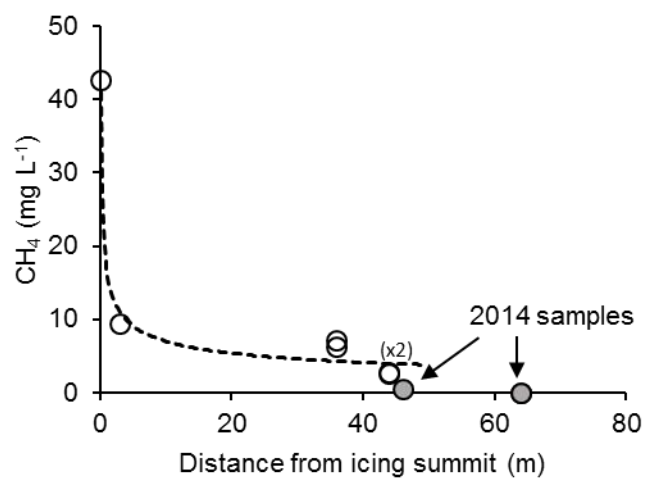
600 **Figure 4.** Histograms showing stable isotope composition of methane and CO₂ in pingo spring waters (from Table 2) for
 601 comparison with published pore gases from different depths at the CO₂ Well Park (Well Site B in Figure 2). The ratio of
 602 methane to the sum of ethane and propane (all in μL mL⁻¹) is shown to indicate where biogenic methane is most likely (i.e.
 603 high values). Also shown are the approximate lower boundary of the permafrost and the aquifer beneath it.

604

a



b



605

606 **Figure 5.** Rapid decrease in dissolved methane concentration with distance from the source of a sub-permafrost groundwater
607 outburst at Innerhytte Pingo summit April 2015.

Date	pH	ORP (mV)	O ₂	$\delta^{18}\text{O}_{\text{H}_2\text{O}}$ ‰ vsmow	$\delta\text{D}_{\text{H}_2\text{O}}$ ‰ vsmow	Cl	NO ₃	SO ₄	DIC	Na	K	Mg	Ca
River Bed Pingo (distal)													
21/4/17	7.18	134	1.1	-15.4	-111	1560	b.d	2880	229	1020	7.89	518	459
5/4/17	7.32	-64.1	0.0	-14.9	-109	1520	b.d	1950	281	916	6.89	353	381
17/3/17	8.15	-25.1	0.0	-15.1	-109	775	b.d	3670	305	563	6.30	537	534
19/3/17	7.22	113	2.2	-15.3	-109	780	b.d	3510	236	539	5.96	495	480
River Bed Pingo													
16/4/16	7.21	-192	0.31	-14.3	-102	1540	0.04	40.1	2700	1910	4.99	13.8	31.6
12/4/16	7.06	-12.1	0.17	-14.0	-101	1510	0.08	43.2	2770	1980	4.95	13.0	30.7
12/4/15	7.61	-74.9	0.68	-13.9	-99.8	1450	b.d	24.3	3710	2270	6.92	20.1	32.6
Innerhytte Pingo													
19/4/17	7.16	-35.4	0.77	-13.7	-99.2	1530	b.d	b.d	2000	1690	4.14	12.7	19.3
15/4/17	7.11	-119	0.0	-13.6	-98.9	1490	b.d	b.d	2023	1680	4.13	11.7	18.4
17/3/17	6.81	-67.4	0.30	-13.6	-99.4	1520	b.d	1.40	2043	1700	4.48	12.3	18.9
21/4/16	6.89	-189	0.43	-14.5	-103	1380	0.03	38.6	3930	2310	3.70	20.6	40.0
12/4/16	7.07	-20.7	0.23	-13.5	-97.6	1410	0.02	14.5	3990	2330	3.54	20.2	39.6
22/4/15	6.88	-20.7	0.22	-13.3	-95.2	1490	b.d	17.4	3870	2360	5.30	17.7	28.1
Førstehytte Pingo													
19/4/17	7.35	-195	1.1	-14.4	-107	1100	b.d	11.3	2430	1580	5.89	13.4	20.4
15/4/17	7.34	-180	0.0	-15.0	-106	1130	b.d	12.1	2390	1580	7.41	15.2	20.1
16/3/17	7.35	-140	0.34	-14.8	-105	1070	b.d	15.6	2360	1540	5.43	13.7	21.1
21/4/16	7.31	-238	0.49	-15.7	-110	1058	0.03	48.5	4180	2190	5.54	21.6	40.7

12/4/16	7.20	-199	0.30	-14.7	-105	1100	0.15	63.7	4130	2210	5.76	21.5	42.0
9/4/16	7.21	-192	0.31	-14.7	-105	1100	0.10	59.3	3870	2110	5.69	21.6	40.9
10/5/15	7.81	-202	0.90	-15.7	-111	1100	b.d	35.0	4540	2340	10.6	23.8	30.8
23/4/14	7.25	-212	0.60	-14.4	-102	1100	b.d	53.9	7560	3430	12.0	25.8	39.6
Lagoon Pingo													
19/4/17	7.9	-229	2.44	-15.1	-108	392	b.d	121	3540	1560	25.4	28.1	12.9
15/4/17	8.05	-202	0.00	-15.2	-108	418	b.d	128	3480	1550	26.3	29.3	13.3
16/3/17	7.71	-181	1.71	-15.5	-108	396	b.d	115	2340	1130	19.7	21.0	9.20
10/4/16	7.94	-207	0.48	-15.2	-106	541	0.05	248	5250	2260	39.2	63.2	38.2

608

609 **Table 1.** Geochemical characteristics of Adventdalen pingo springs during pre-melt season sampling. All units are in mg L⁻¹

610 unless otherwise stated. NO₃ is reported as mg-N L⁻¹ and “b.d” means “below detection” (ca. 0.02 mg L⁻¹).

611

Date	CH ₄ (mg L ⁻¹)	eCO ₂ (mg L ⁻¹)	δ ¹³ C-CH ₄ (‰ VPDB)	δ ¹³ C-DIC (‰ VPDB)
River Bed Pingo (<u>distal</u>)				
21/4/17	4.78	19.6	-54.4	12.6
5/4/17	6.23	17.3	-55.0	12.5
17/3/17	0.61	2.36	b.d.	10.1
19/3/17	0.97	18.9	b.d.	10.1
River Bed Pingo				
16/4/16	32.4	221	-55.6	n.d.
12/4/16	24.9	320	-51.5	n.d.
12/4/15	20.2	121	-55.9	n.d.
Innerhytte Pingo				
<u>23/9/17</u>	<u>25.0</u>	<u>183</u>	<u>-53.8</u>	<u>27.1</u>
19/4/17	31.4	208	-55.9	26.7
15/4/17	27.6	420	-56.1	12.6
17/3/17	30.0	672	-55.7	26.3
21/4/16	41.3	451	-57.8	n.d.
12/4/16	42.6	678	-51.8	n.d.
22/4/15	25.0	183	-49.7	n.d.
Førstehytte Pingo				
<u>3/10/17</u>	<u>11.9</u>	<u>641</u>	<u>-64.2</u>	<u>2.5</u>
<u>13/9/17</u>	<u>16.5</u>	<u>770</u>	<u>-64.7</u>	<u>2.7</u>
19/4/17	15.3	143	-48.2	1.7
15/4/17	15.1	145	-52.3	2.4
16/3/17	14.0	139	-54.0	2.4
21/4/16	18.1	271	-67.4	n.d.
12/4/16	14.1	346	-55.3	n.d.
9/4/16	16.6	317	-56.1	n.d.
10/5/15	13.4	93.0	-67.1	n.d.
Lagoon Pingo				
<u>28/9/17</u>	<u>7.26</u>	<u>210</u>	<u>-70.7</u>	<u>-8.4</u>
<u>24/8/17</u>	<u>9.50</u>	<u>58.7</u>	<u>-69.8</u>	<u>n.d.</u>
19/4/17	6.30	40.7	-55.6	n.d.
15/4/17	9.63	60.1	-48.3	n.d.
16/3/17	13.7	79.6	-62.0	n.d.
10/4/16	9.50	58.7	-66.8	n.d.

612 **Table 2.** $\delta^{13}\text{C}$ composition and concentration of methane and dissolved inorganic carbon (DIC) in pingo springs. “eCO₂” is
 613 the excess of CO₂ relative to equilibrium with the atmosphere. Samples collected opportunistically during the summer are
 614 underlined, “n.d.” means “not determined, whilst “b.d.” means results were below the detection limit.

615
 616

Source	Spring discharge (L s ⁻¹)	Average CH ₄ concentration (Mg L ⁻¹)	Annual CH ₄ Flux (kgCH ₄ y ⁻¹)
River Bed Pingo	0.11*	25.8	89.6
Innerhytte Pingo	0.29**	31.8	291
Forstehytte Pingo	0.46**	15.0	218
Lagoon Pingo	0.26**	9.3	76.4
Lagoon Lake	0.52**	22.9	376
Total	1.64	20.2	1051
Active layer emissions			6040 - 10400

617
 618
 619
 620
 621
 622
 623
 624

Table 3. Sub-permafrost groundwater discharge and CH₄ flux estimates. ~~The atmospheric flux is the sum of all separate flux except that discharging into the sea (“Fjord”), which is uncertain and assumed to be oxidised.~~ Active layer emissions are median annual fluxes from individual chambers, reported by Pirk et al (2017). (Source: *Hornum et al (In Review); **authors’ own measurements).